J. Earth Syst. Sci. (2022)131 136
https://doi.org/10.1007/s12040-022-01878-1

Assessment of climate change of different meteorological state variables during Indian summer monsoon season

R Bhatla[1,2,*], Archana Maurya[1], Palash Sinha[3], Shruti Verma[1] and Manas Pant[1,2]

[1]*Department of Geophysics, Institute of Science, Banaras Hindu University, Varanasi, India.*
[2]*DST-Mahamana Centre of Excellence in Climate Change Research, Institute of Environment and Sustainable Development, Banaras Hindu University, Varanasi, India.*
[3]*School of Earth, Ocean and Climate Sciences, Indian Institute of Technology, Bhubaneswar, India.*
**Corresponding author. e-mail: rbhatla@bhu.ac.in*

MS received 23 July 2021; revised 7 January 2022; accepted 23 January 2022

Long-term assessment of basic meteorological field variability is an important factor that influences the Indian summer monsoon and consequently affects the socio-economic aspects of India. In this study, the spatial and temporal variation of meteorological parameters during summer monsoon season using NCEP/NCAR reanalysis datasets for the period of 70 years (1948–2017) has been analyzed in climatology, early-late phase and multidecadal epochs over India and its regions. Statistical techniques such as the standardized anomaly index of surface temperature, rainfall and zonal and meridional wind (at 850 and 200 hPa) and temporal analysis of Mann–Kendall trend test over six selected regions, *viz.*, North India (NI), Central India (CI), Southern India (SI), Arabian Sea (AS), Bay of Bengal (BoB) and Equatorial Indian Ocean (EIO) reveal higher variability during summer monsoon season from 1948 to 2017. The significant spatial changes in the value of standard deviation and coefficient of variation confirm the early-late phase and multidecadal modulation of the seasonal variability of selected climatic parameters. The results indicate that the escalation in the surface temperature multidecadal variability and trend has dominating characteristics over NI, CI and SI regions at an alarming range (0.5–1.0°C). The major hotspots of increasing early-late phase and multidecadal variability and average precipitation have been found over BoB, EIO and SI ($\sim$1–3.5 mm/day). The decreasing changes in the mean rainfall pattern and associated variability is strongly linked with increasing surface warming and significant reduction in the strength of surface zonal wind over BoB, IO, SI and CI region which cause the weakening of important atmospheric circulations such as the role of Somali jet and strong low-level jet (LLJ) during Indian summer monsoon season. Also, the meridional wind at the surface and upper level has shown significant enhancement over AS and EIO. The recent decadal anomaly (2008–2017) is really a matter of concern as precipitation and wind circulation anomaly at 850 and 200 hPa have shown decreasing trends over all the regions. In recent years, the variation in meteorological parameters and distribution are asymmetrical during summer monsoon season in changing climate.

Keywords. Meteorological parameters; monsoon variability; NCEP/NCAR; Mann–Kendall test.

Published online: 03 June 2022

1. Introduction

The Indian Summer Monsoon Rainfall (ISMR) is one of the most intense climatic elements yet its initiation and variations are not well established (Rajeevan *et al.* 2000; Turner and Annamalai 2012). The ISMR has major dominance and its contribution is about 75–80% of the total annual rainfall of the country, play a vital role in the economy of Indian agriculture (Parthasarathy *et al.* 1994; Guhathakurta and Rajeevan 2008). The monsoon is associated with large-scale seasonal reversal of pressure, temperature and winds, also accompanied by changes in precipitation with heavy rain during the summer monsoon (Goswami *et al.* 1999; Krishnan *et al.* 2013). Low-level jet (LLJ) stream is a very important component to drive monsoon and wind transport provides large quantities of moisture to the Indian subcontinent and most of its annual rainfall (Joseph and Sijikumar 2004; Naidu *et al.* 2011; Aneesh and Sijikumar 2016).

Several studies found that variation of ISMR on decadal to multidecadal has the presence of 60-year cycle in it (Krishnamurthy and Goswami 2000). A detailed study of long-reconstructed time series of ISMR brings out a statistically significant 50–80-year multidecadal mode of variability (Mohanty *et al.* 2002; Swapna *et al.* 2017). The potential factors which cause the decadal to multi-decadal scale variability of the ISMR are Pacific decadal oscillation (PDO) and Atlantic multi-decadal oscillation (AMO) (Bhatla *et al.* 2013, 2020; Malik *et al.* 2017). The multidecadal mode provides significant modulation of interannual variability. The year-to-year (interannual) variability of monsoon rainfall has been studied by many researchers during the past six decades (Mooley and Parthasarathy 1984; Krishnamurthy and Shukla 2008). The rainfall study encloses several prospects like linear trends, epochal variations and teleconnections with the El Nino southern oscillation (ENSO), Indian Ocean dipole (IOD) (Gadgil *et al.* 2004; Krishnan *et al.* 2013; Han *et al.* 2014; Sinha *et al.* 2015). Precipitation is a highly variable meteorological parameter both temporally and spatially. Due to the impact of climate changes, there are significant changes in the mean rainfall pattern and their variability (Kothawale *et al.* 2010; Guhathakurta *et al.* 2015). In recent studies by Huang *et al.* (2020), it was concluded that the revival of monsoonal precipitation is not just an inter-decadal variation and will last for multiple years. This apparent revival of summer monsoon precipitation is closely associated with a favourable land–ocean temperature gradient, driven by a strong warming signature over the Indian subcontinent. The spatio-temporal distribution of surface temperature and precipitation over a given region results from several complex causes and interacting processes. During Indian summer monsoon (ISM), variations in surface temperature and precipitation distribution to discern major seasonal regimes and their forcing mechanisms, by examining distribution from a statistical perspective (Ananthakrishnan and Soman 1989; Trenberth 2011; Mishra *et al.* 2020b; Kumari *et al.* 2021) rather than from a purely climatological one. Despite the large evidence of increasing temperatures all over the world, accurate estimation of the time trends is still an open issue. The structure of the oceanic mixed layer in BoB as well as AS is a key factor that influences climatological aspects of ISMR. In other respects, AS also contributes major role during monsoon season and several researchers investigated the effect of AS with monsoon events (Levine *et al.* 2013; Mishra *et al.* 2020a). As the agricultural productivity and freshwater resources of each region are strongly dependent on monsoon rainfall, it is crucial to understand the causative mechanisms responsible for these regional trends of monsoon rainfall for planning agricultural productivity and water resource management. A recent study stated that anthropogenic aerosols are a potential driver for either increasing or decreasing monsoon rainfall (Guo *et al.* 2016; Li *et al.* 2016). Thus, asymmetry in trends of precipitation and increasing/decreasing trend of the large continental-scale culpable may be due to dynamics of ISM.

The spatio-temporal distribution and variation of ISMR are dependent on many climatic and topographical features over the Indian subcontinent (Parthasarathy *et al.* 1994; Gadgil 2000; Goswami 2006; Rajeevan *et al.* 2007). The objective of this study is to examine the behavior of climate change impact on different meteorological state variables during ISM season and how it impacts both spatially and temporally at different regional scales. The analysis of variation of meteorological parameters during ISM is of great importance for researchers and policy makers in their decision making as rainfall, temperature and

wind at 850 as well as 200 hPa plays dominant role in deciding the use of the water availability, extreme events and global warming in changing climate.

2. Data and methodology

In the present study, the 70-year (1948–2017) reanalysis datasets from National Centre for Environmental Prediction/National Centre for Atmospheric Research Reanalysis (NCEP/NCAR) at 2.5° × 2.5° horizontal resolution has been chosen to provide a consistent and reliable analysis for the variation of different meteorological parameters for investigating dynamics during summer monsoon in changing climate over Indian region (40°N–10°S and 20°–110°E). This dataset is preferred over other reanalysis data as it offers longer period of availability with multiple meteorological state variables at the same source to understand the variability of monsoon climate in epochal and inter-decadal from 1948 to 2017 (NCEP; https://psl.noaa.gov/data/gridded/data.ncep.reanalysis.html) (Kalnay *et al.* 1996). These datasets have been generally used in several spatio-temporal climate studies (Yanai and Tomita 1998; Kistler *et al.* 2001; Sahana *et al.* 2015). The variation of meteorological parameters in changing climate is concerned with the variability in the mean state and other statistics. In this study, average and multi-decadal anomalies have been analysed using the reanalysis datasets. Along with this, to prove the influence of climate change on summer monsoon during late and early phase, i.e., 1948–1982 (T1) and 1983–2017 (T2), analysis has been performed which is mentioned as T1 and T2, respectively.

The composite analysis usually involves computing the composite mean and other statistical measures such as standard deviation (Std), coefficient of variation (CV) for statistical significance as well as fluctuation features of the regions, *viz.*, North India (NI; 72–87°E, 24–28.5°N), Central India (CI; 73–84°E, 18.5–23.5°N), Southern India (SI; 75–80°E, 7.9–17°N), Arabian Sea (AS; 52–74°E, 6–15°N), Bay of Bengal (BoB; 82–95°E, 6.5–17°N) and Equatorial Indian Ocean (EIO; 48–95°E, 7°S–5°N). The CV measures the overall variability of the rainfall in the area of interest and a lower (higher) value of CV indicates less (more) rainfall variability. To analyse the time series, standardization procedure has been utilized (Kraus 1977). Where the standardized anomaly for temperature and precipitation is defined as:

$$A = \frac{X - \mu}{\sigma}, \tag{1}$$

where X is the average surface temperature or rainfall during monsoon season; μ and σ are the mean and Std of the desired series respectively.

2.1 *Trend analysis*

2.1.1 *The Mann–Kendall test*

The Mann–Kendall (M–K) trend test is generally used in several studies for trend analysis in climatological time series data (Gocic and Trajkovic 2013). Consequently, the statistical significance and trends of these selected regions were examined by temporal M–K trend test (Mann 1945; Kendall 1975) at the 90 and 95% confidence level together with Sen's slope. M–K trend test is a nonparametric test and its statistics (S) with standardized statistics (Z) are given as:

$$S = \sum_{i=1}^{n-1} \sum_{j=i+1}^{n} \operatorname{sign}(X_j - X_i), \tag{2}$$

$$\operatorname{sign}(X_j - X_i) = \begin{cases} +1, & \text{if } (X_j - X_i) > 0 \\ 0, & \text{if } (X_j - X_i) = 0 \\ -1, & \text{if } (X_j - X_i) < 0, \end{cases} \tag{3}$$

$$Z = \begin{cases} \dfrac{S-1}{\sqrt{\mathrm{VAR}(S)}} & \text{if } S > 0 \\ 0 & \text{if } S = 0 \\ \dfrac{S+1}{\sqrt{\mathrm{VAR(S)}}} & \text{if } S < 0, \end{cases} \tag{4}$$

$$V(S) = \frac{1}{18}[n(n-1)(2n+5) - \sum_{p=1}^{q}(t_p - 1)(2t_p + 5)], \tag{5}$$

where X_i and X_j are the time-series observations, n is the length of the time series, t_p is the number of ties for pth value, and q is the number of tied values. Positive Z indicates an increasing trend, whereas negative Z indicates a decreasing trend in the time series.

2.1.2 *Sen's slope*

Sen (1968) investigated a simple non-parametric procedure to find the true slope with detection

of linear trend in the time series which is defined as:

$$f(t) = Qt + B, \tag{6}$$

where Q is slope and B is a constant.

The slopes of all data pairs are calculated as:

$$Q_i = \frac{x_j - x_k}{j - k},\ i = 1, 2, \ldots, N,\ j > k. \tag{7}$$

The median of these N values of Q_i gives us Sen's estimator of the slope. These N values are ranked in increasing order. Sen's estimator of the slope is given as:

$$Q = \begin{cases} Q_{\frac{N+1}{2}}, & \text{if } N \text{ is odd} \\ \frac{1}{2}\left(Q_{\frac{N}{2}} + Q_{\frac{N+2}{2}}\right), & \text{if } N \text{ is even} \end{cases}. \tag{8}$$

To find if the Q value (trend) is statistically different from zero, confidence level of the value is obtained at a specific probability.

2.1.3 *Student's t-test*

Student's t-test is one of the prominent test methods for studies of long-term variations of the climate system (Kripalani and Kulkarni 1997; Bhatla *et al.* 2016). Here we have applied the statistically significant t values above 99% level of significance and contoured in the difference of late and early phases plots. The critical value of student's t-test with a 0.01 significance level is 2.65. The following formula is used for calculating t-value and degrees of freedom in student's t-test:

$$t = (X_1 - X_2)/\sqrt{S_p^2\left(\frac{1}{n_1} + \frac{1}{n_2}\right)}, \tag{9}$$

$$S_p = \sqrt{\left\{(n_1 - 1)S_{x_1}^2 + (n_2 - 1)S_{x_2}^2\right\}/(n_1 + n_2 - 2)} \tag{10}$$

where X_1 and X_2 are the average value of different epochs, n_1 and n_2 are the total no. of years in each epoch, S_{x_1} and S_{x_2} correspond to the Std of X_1 and X_2, respectively. The degrees of freedom $= (n_1 + n_2 - 2)$.

3. Results and discussion

In the present section, composites of climatological mean and epochal changes of basic meteorological parameters over Indian region (30°S–40°N; 30°–110°E) during summer monsoon (JJAS) season have been discussed. For that purpose, the variation of parameters namely surface pressure, surface temperature at 2 m, precipitation, zonal and meridional wind (at 850 and 200 hPa), cloud cover and outgoing longwave radiation (OLR) have been considered. The spatio-temporal variation of these parameters has been divided into various time slices, i.e., average of 70 years (1948–2017), late/early phase and multi-decadal which are being discussed below.

3.1 *Climatology and epochal changes of surface pressure*

The spatio-temporal distribution of surface pressure has been represented in figure 1 where figure 1(a) shows 70 years of mean during monsoon season (JJAS). A low-pressure pattern was observed over western part of India and adjoining region, southern region and increases over Indo-Gangetic plain (IGP) region (990–1010 hPa). The variation of surface pressure during monsoon trough over AS having some regions higher pressure than BoB above 1010 hPa, the southern region shows a significant reduction in rainfall. Further, pressure anomaly between two T2–T1 is shown in figure 1(b) having consistent pattern of pressure anomaly; distribution of pressure anomaly increases significantly from south to north part of Indian landmass (more positive anomaly) and the blue contour lines represent statistically significant at 99% confidence level. Figure 1(c and f) reveals negative pressure anomalies on the entire part of Indian region and EIO (negative pressure anomaly), whereas figure 1(d and e) have more positive anomaly all over the Indian region. Further, figure 1(g) also depicts negative pressure anomaly (–20 hPa) over southern, north-east part, BoB and positive pressure anomaly (20–40 hPa) over northern part, while in central region minimum positive anomaly (10 hPa) is observed. Figure 1(h) shows negative anomaly everywhere except Himalayan and Tibetan region, maximum negative anomaly (–40 to –60 hPa) found over IGP region. Since monsoons are associated with large-scale seasonal reversals of pressure, several studies tried to establish the linkage between the epochal changes in surface pressure with other meteorological parameters (Krishnan *et al.* 2011; Karmakar *et al.* 2017; Vidya *et al.* 2020).

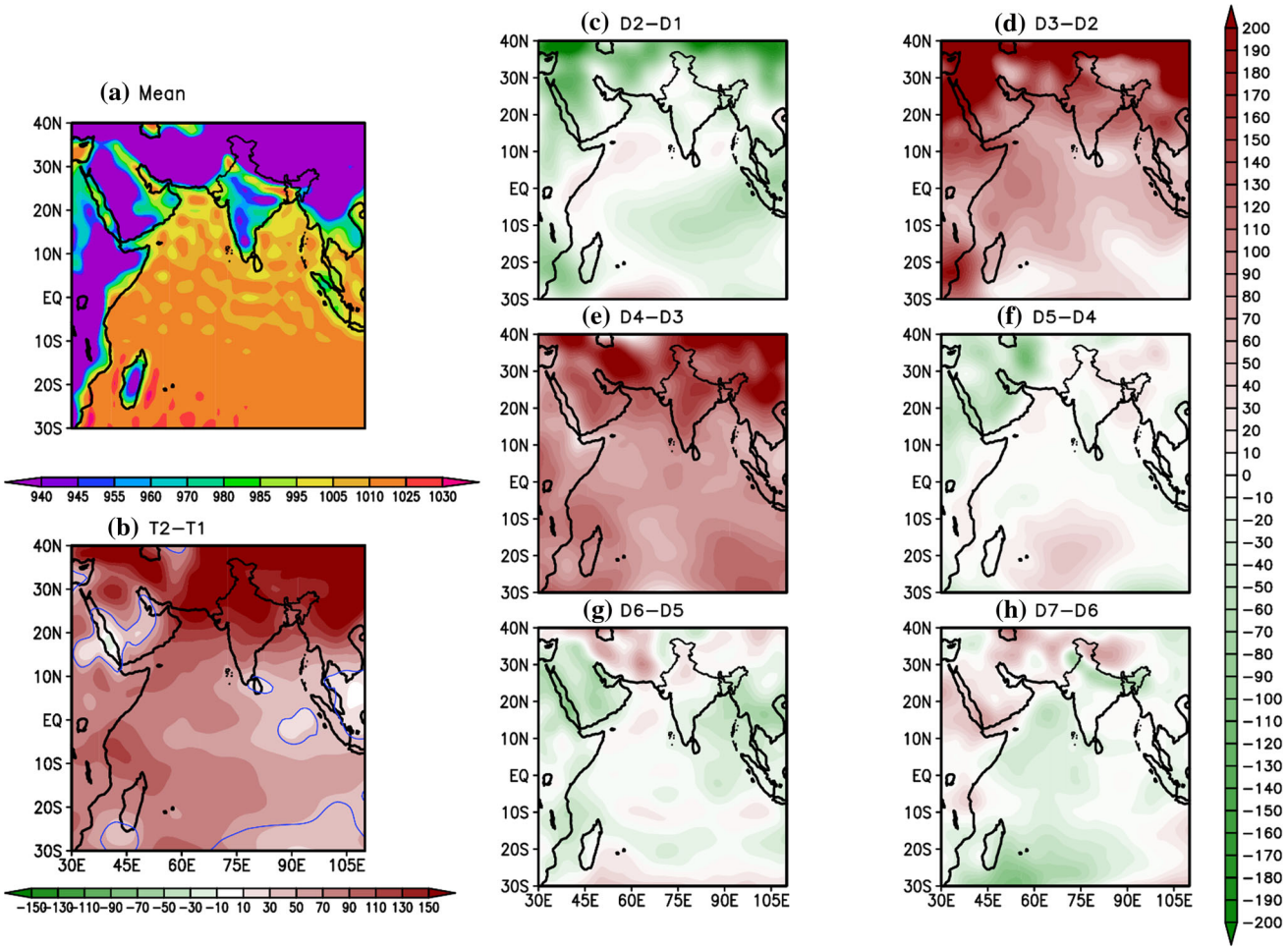

Figure 1. Geographical distribution and epochal changes of surface pressure (units are in hPa) using NCEP reanalysis data for June–September (JJAS) from 1948 to 2017. **(a)** Mean surface pressure (hPa), **(b)** difference in surface pressure between the recent (T2; 1983–2017) and previous (T1; 1948–1982) epochs, **(c)** decadal changes of surface pressure between second (D2; 1958–1967) and first (D1; 1948–1957) decades, **(d–h)** are same as (c) but computed using third (D3; 1968–1977) and second, fourth (D4; 1978–1987) and third, fifth (D5; 1988–1997) and fourth, sixth (D6; 1998–2007) and fifth, seventh (D7; 2008–2017) and sixth decades, respectively. Blue contours in (b) indicate regions with statistically significant changes at 99% confidence level.

3.2 *Climatology and epochal changes of temperature*

The average air temperature at 2 m during ISM season (figure 2a) depicts the maximum mean temperature in the range 34–36°C over north-western part of India, while temperature in the range 28–32°C has been reported over northern Indian regions. This maximum temperature over north-west India may be due to the desert area west of Aravallis which receives low rainfall, low humidity and high-velocity winds. Also, western coastal regions and southern Indian regions depicted 22–24°C and 24–26°C respectively, whereas the rest of India (north-eastern, central and some part of southern regions) reported temperature 26–28°C. Further, BoB region was found to be warmer (28–30°C) than AS (26–28°C) because during monsoon season (JJAS), winds are stronger and support the change of heat to deeper layers owing to overturning and turbulent mixing (Shenoi *et al.* 2002). It can also be observed that Northern IO surface temperatures are warmer, along with the plains of northern India and Tibetan Plateau. The temperature difference between T2 and T1 during 1948–1982 (T1) and 1983–2017 (T2) has been shown in figure 2(b), contoured regions are statistically significant at 99% confidence level which depicts positive anomaly all over Indian region except some parts of J & K, Northeast India and adjoining region of Pakistan and Nepal where negative anomaly has been reported. Further, positive anomaly increases over southern India, from 0.6 to 0.8°C and maximum positive anomaly has been observed over Tibetan Plateau (1.2–1.4°C). A warming pattern (positive anomaly)

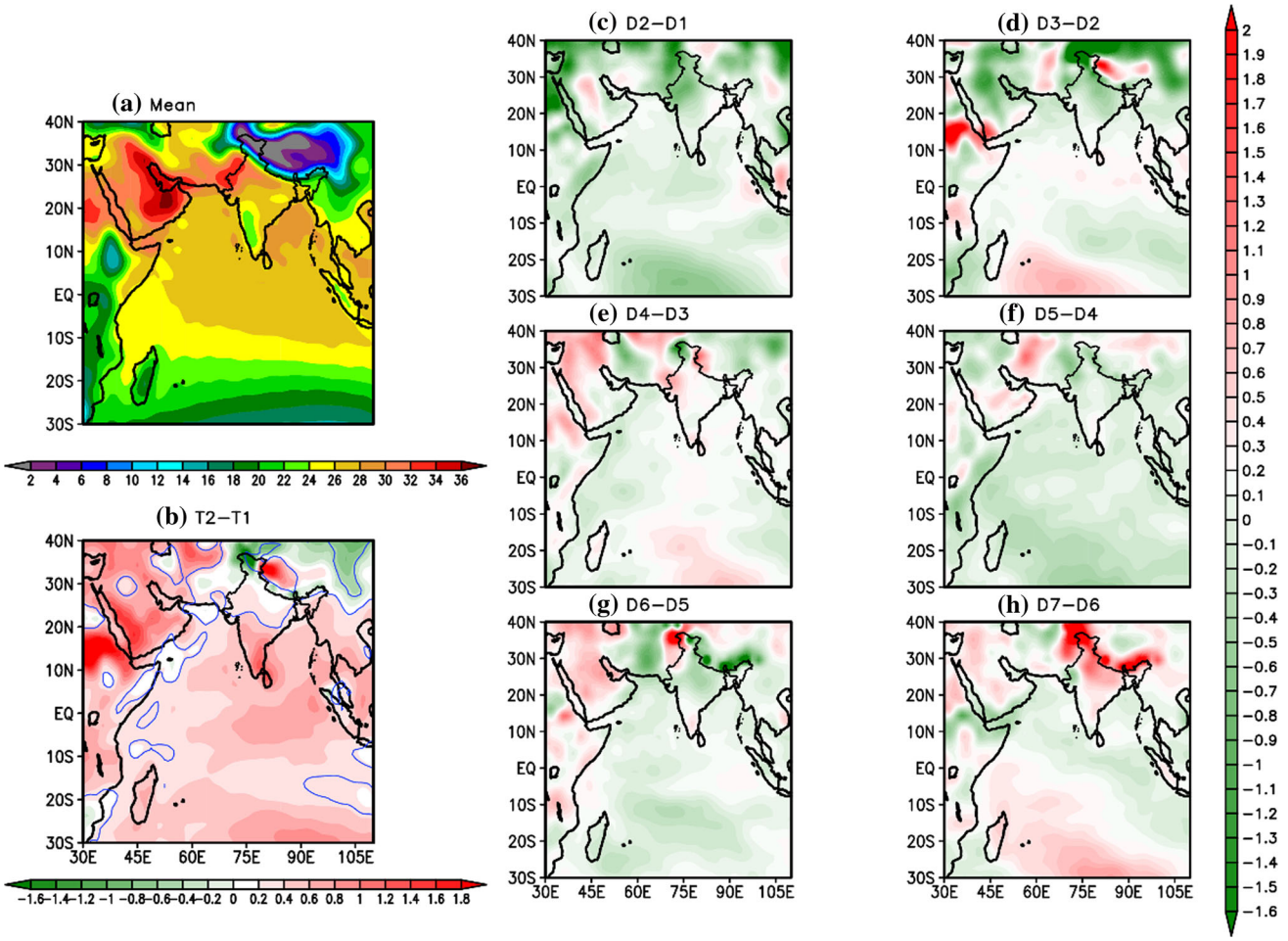

Figure 2. (**a–h**) Same as figure 1, but computed for surface temperature at 2 m (T2m) (units are in °C).

has been observed as far as northwestern Indian region is concerned, while a cooling pattern (negative anomaly) was reported over northeastern and central Indian regions.

The decadal anomalies of surface temperature have been shown in figure 2(c–h), which suggests that global warming is manifesting itself over India and its regions. In figure 2(c–g), negative anomalies have been observed everywhere except topmost part of northern India. Some southern regions and BoB region depicted more positive temperature anomaly from 0.4 to 0.6°C. Further in figure 2(h), more positive anomaly between 0.6–0.8°C and 1.2–1.4°C over northcentral and north-eastern part of India can be depicted. Further, a pattern of global warming is observed as sea surface temperature plays an important role to understand the variability of ISM. Minimum temperature was found over Tibetan region and this may be due to snow cover and a weakening in the sensible heat source over the Tibetan Plateau (Duan *et al.* 2013; Curio *et al.* 2019). Warming pattern over southern region and cooling pattern over northeastern and central regions are perfectly explained by several researchers (Dong *et al.* 2016; Li *et al.* 2016; Ross *et al.* 2018). Due to the presence of anthropogenic haze (aerosol pollution) over southeast Asia, India and adjoining ocean region absorbed solar energy which leads to warming of haze in these regions and results in cooling of the surface air.

3.3 *Climatology and epochal changes of precipitation*

The variation of precipitation in the context of climate change during summer monsoon season (JJAS) is mainly constrained by rainfall activity and climatology of precipitation. It can be better understood with the help of surface temperature and pressure from 1948 to 2017. The spatial distribution of precipitation (figure 3a), the mean

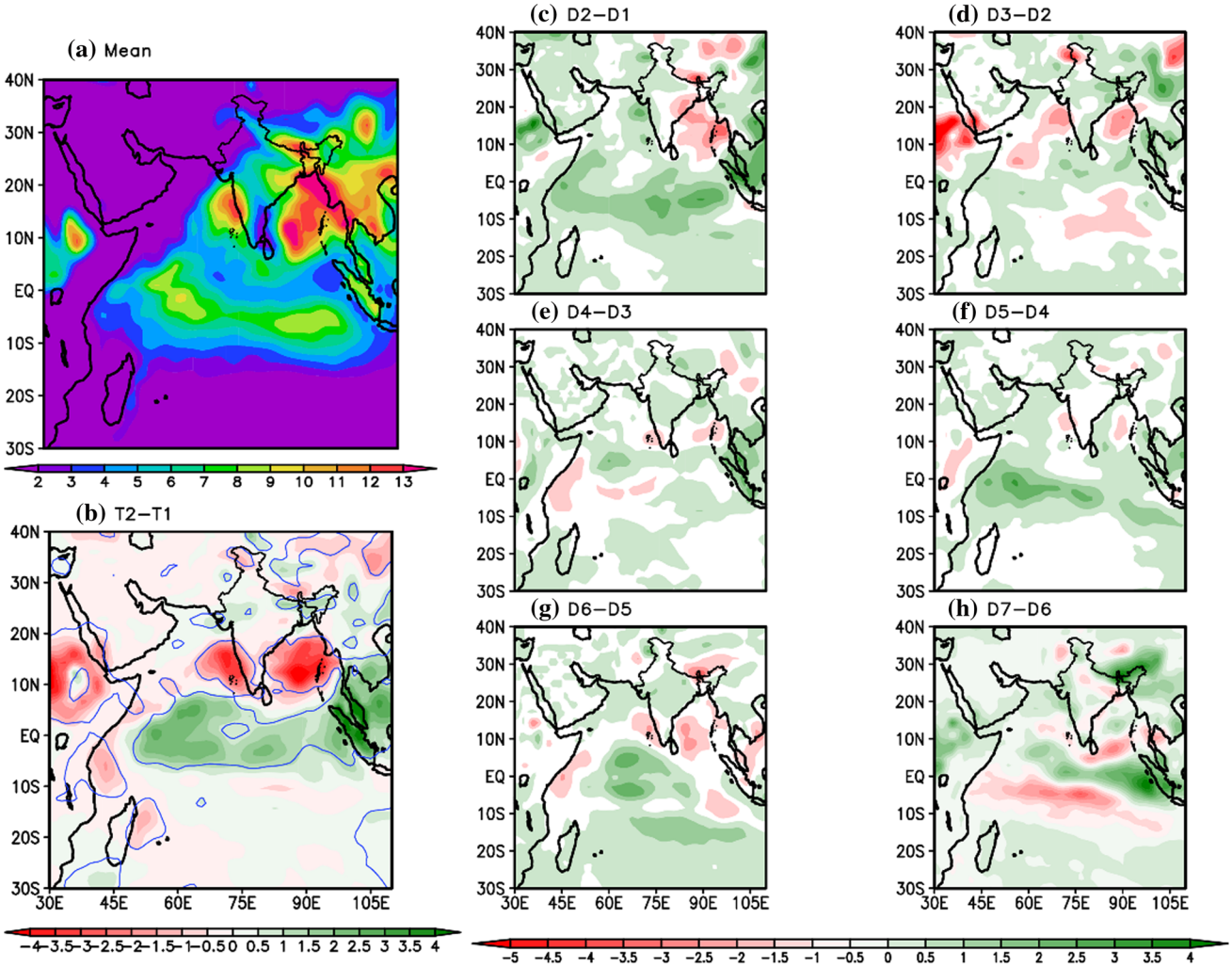

Figure 3. (**a–h**) Same as figure 1, but computed for precipitation (units are in mm/day).

precipitation rate depicts higher rainfall over west of Western Ghats, northeast region, BoB and adjoining regions between 11–12 and 12–13 mm/day respectively, while low rainfall over the leeward side of south India and the gradual increase from east to west over central and north India leads to desert-like conditions in northwestern region. The early and late phase precipitation anomaly (T2–T1) (figure 3b) and contoured regions reveal statistically significant at 99% level with positive anomaly (1–2 and 2–3 mm/day) over entire continental part of India and EIO. Whereas the Western Ghats, adjoining region of AS and some parts of BoB have significant negative anomaly. Further, figure 3(c–h) represents an inconsistent pattern of decadal anomaly as negative precipitation anomaly from –2 to –2.5 mm/day observed over northeastern part, West Bengal and some part of the southern region and increase over EIO (5°N–5°S) from 1 to 1.5 mm/day. Positive precipitation in decadal anomaly observed over northern India region, Western Ghats and AS from 0.5 to 1.0 mm/day and adjoining regions which also show decrease amount of rainfall in present epoch, while rest of India reveals very low anomaly from –1 to 0.5 mm/day. Major changes of decadal precipitation anomaly observed over AS, BoB, EIO (5°N–5°S), central India including IGP and Western Ghats of peninsular India. The comparison of temporal variation of precipitation and temperature anomalies observed a general increase. The distribution of monsoon rainfall is greatly influenced by a number of weather systems, such as the Arctic Oscillation, Siberian High and Western Pacific Subtropical High, as well as the complex Asian topography (Tibetan Plateau), well explained by Loo *et al.* (2015). This observation reveals spatially varying mixed

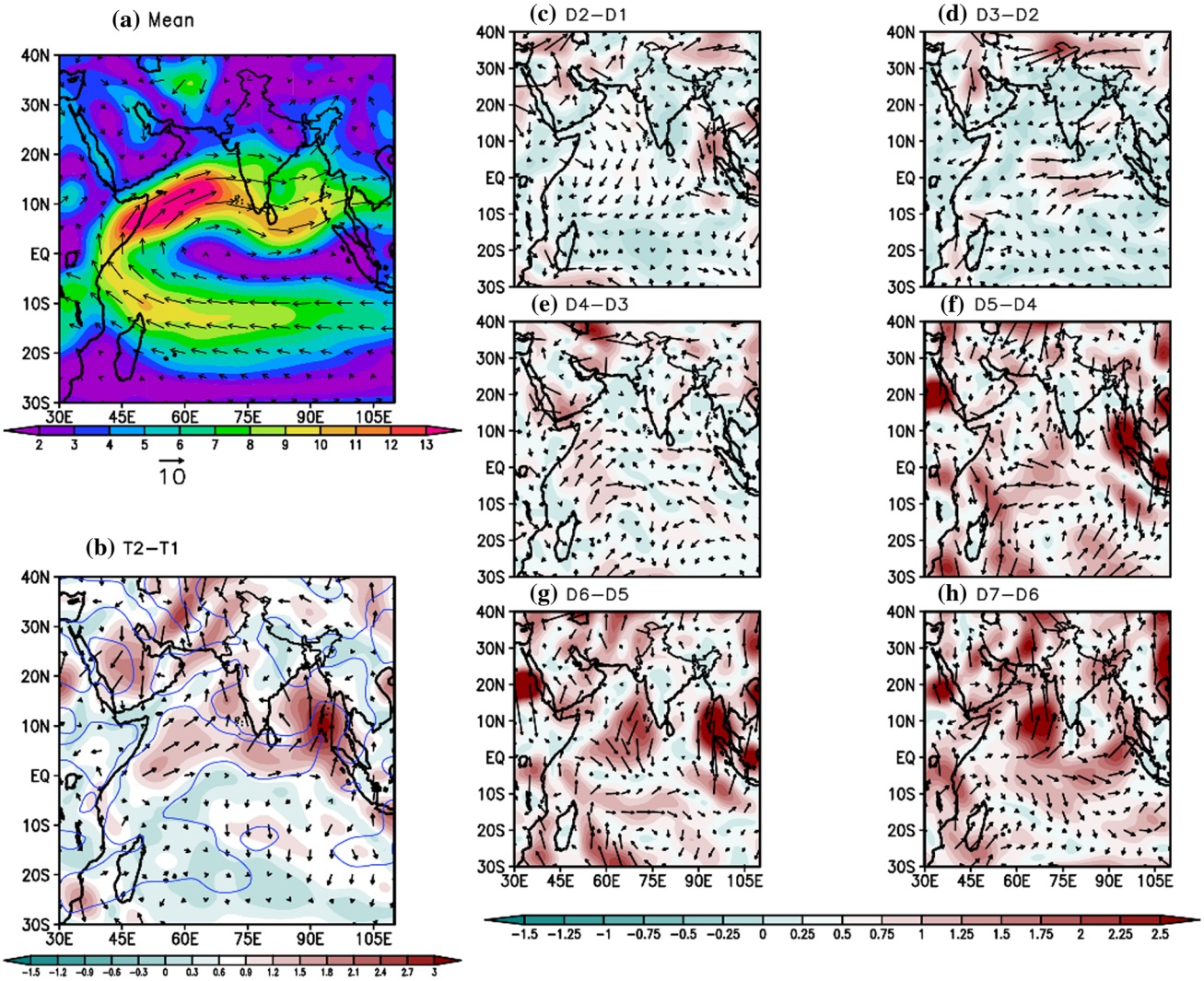

Figure 4. (**a–h**) Same as figure 1, but computed for zonal and meridional winds (u and v components) at 850 hPa (units are in m/s).

responses of global warming towards rainfall occurrence and amounts all over India. The spatial variation of the summer monsoon precipitation over the Indian region is linked to that of the convection over the BoB and AS. There is an increasing trend in the inconsistency of daily rainfall activity due to an increase in the frequency of extreme events in the global warming era (Singh *et al.* 2015). The rise in rainfall and monsoon circulation may be due to an increasing inconsistency of the strength of low-level jet, an increase of sea surface temperature over AS. The positive/negative rainfall anomaly and occurrence for some regions of India are not only due to climate change, but also due to the spatial variability of local changes such as rapid urbanization, industrialization and deforestation.

3.4 *Climatology and epochal changes of surface wind*

One important feature of the south-westerly winds during the summer monsoon season is the low-level westerly jet over the central AS. The southwesterly flow across south and central India and north BoB turn into south easterlies in the sub-Himalayan north India, creating a large-scale low-level cyclonic vorticity (the monsoon trough). These diurnal changes in monsoon winds modulate the moisture convergence process and the associated evolution of rainfall over India. Figure 4 represents the composite wind patterns at 850 hPa pressure level, early-late phase and decadal anomaly using NCEP reanalysis data during Indian monsoon season. The mean composite of wind (figure 4a) depicts very

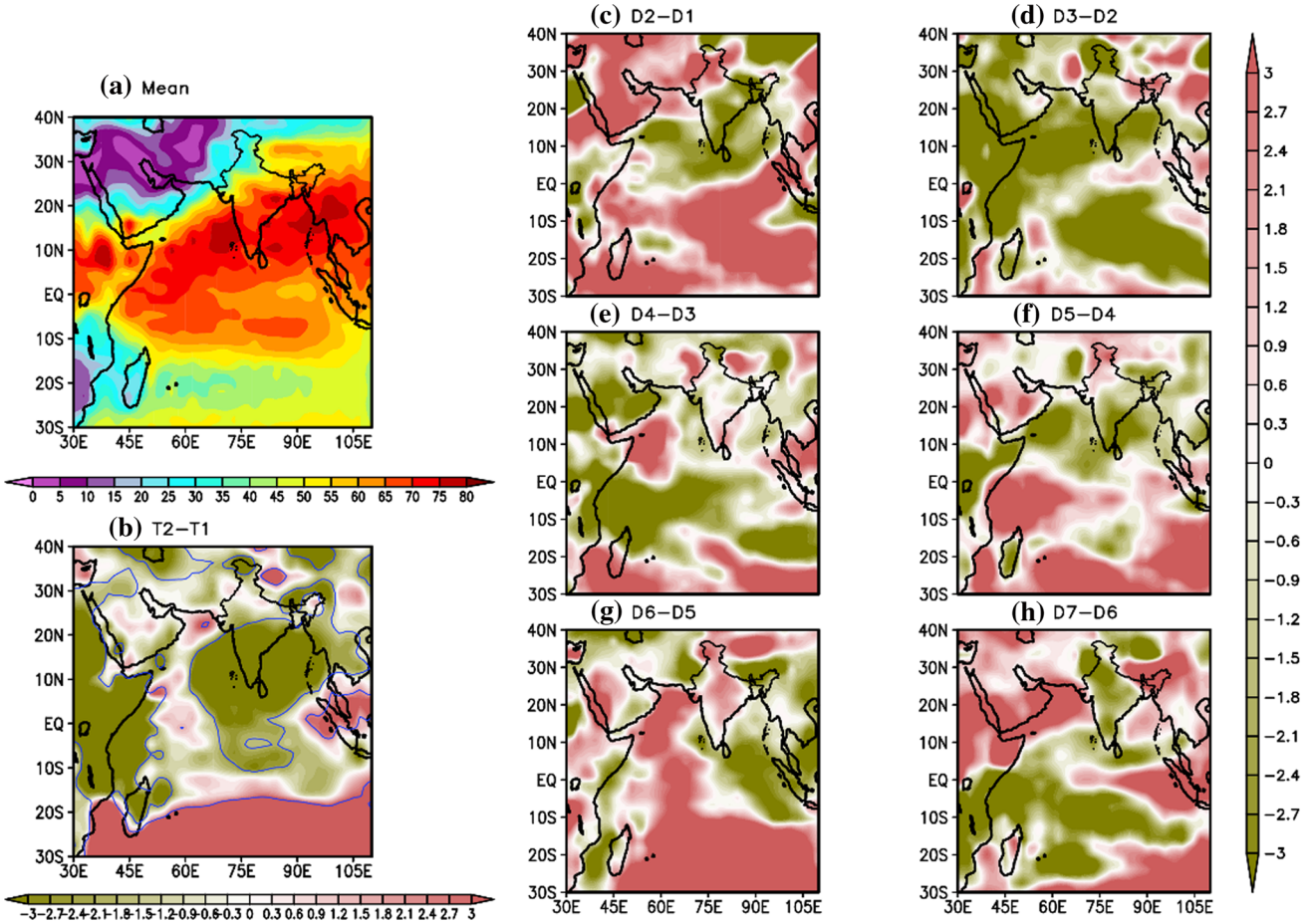

Figure 5. (**a–h**) Same as figure 1, but computed for cloud cover (%).

intense southwesterly wind over Somali region (LLJ) which is associated with the movement of Inter-tropical Convergence Zone (ITCZ). This situation supports the propagation of monsoon circulation over BoB and AS consequently rise in rainfall (Swapna *et al.* 2017). The BoB branch plays an important role over central and southern India, while Arabian branch dominates northeast India, IGP and Bangladesh. Increasing convective activity in the BoB induces stronger winds in the AS and enhances the advection of moisture over India, leading to increased precipitation and strength of the monsoon. The maximum wind speed found over ocean region (13 m/s) brought moisture for rainfall, while wind speed intensities decrease (4–5 m/s) over central and north India. The western southern region is associated with abundant moisture from the south-westerly winds than over IGP, the monsoon precipitation is higher over southern India and decreases towards the northern parts of India which results in stronger zonal winds over AS. From figure 4(b), early-late phase wind anomaly shows stronger monsoon cross-equatorial flow with stronger cyclonic anomalies over south and contoured regions are statistically significant at 99% confidence level. In the oceanic region over EIO (10°S–5°N) near eastern coast of Africa and AS, significant stronger positive anomalies were observed due to intense moisture-laden wind. Further multidecadal anomalies of wind vector from figure 4(c–h) during summer monsoon season show a significantly increasing pattern of anomalies found in recent decadal anomalies due to the presence of strong westerly, southeasterly and southerly anomalies over the EIO, BoB, AS and adjoining region. With the association of spatial plots of pressure, temperature and precipitation rate, they play an important role to understand the distribution of wind magnitude anomaly.

3.5 *Climatology and epochal changes of cloud cover*

Cloud cover affects the temperature due to the effect of cloud in reflecting and absorbing incoming visible solar radiation and outgoing infrared

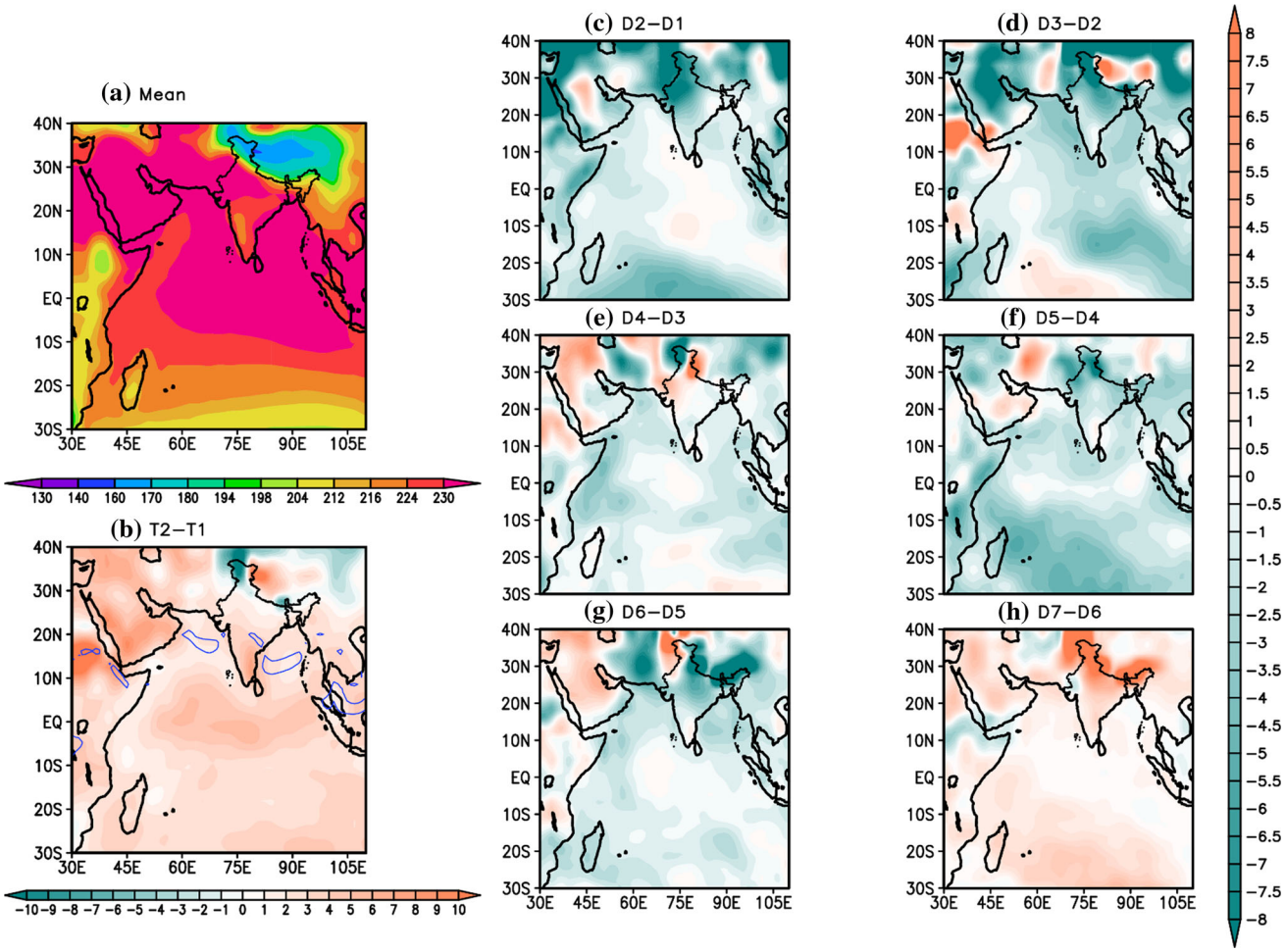

Figure 6. (**a–h**) Same as figure 1, but computed for outgoing longwave radiation (OLR) (units are in W/m^2).

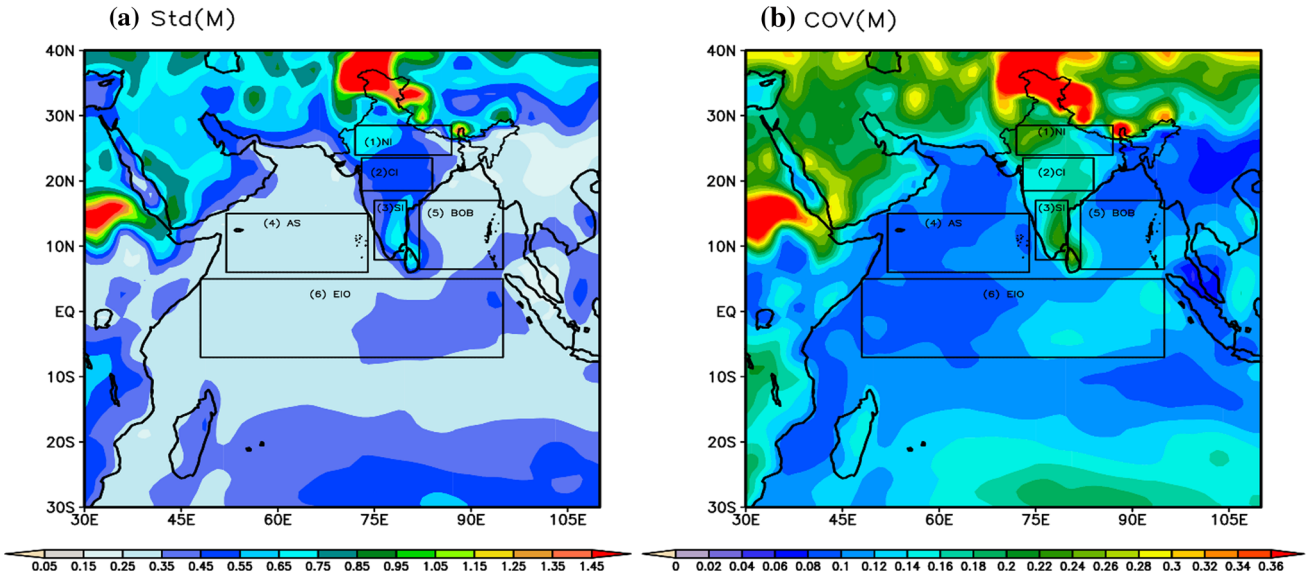

Figure 7. Composite of surface temperature at 2 m (T2m) variability during monsoon season from 1948 to 2017. **(a)** Standard deviation (Std) (units are in °C) and **(b)** coefficient of variation (COV) in % over six selected regions. (1) North India (NI), (2) Central India (CI), (3) Southern India (SI), (4) Arabian Sea (AS), (5) Bay of Bengal, and (6) Indian Ocean (IO).

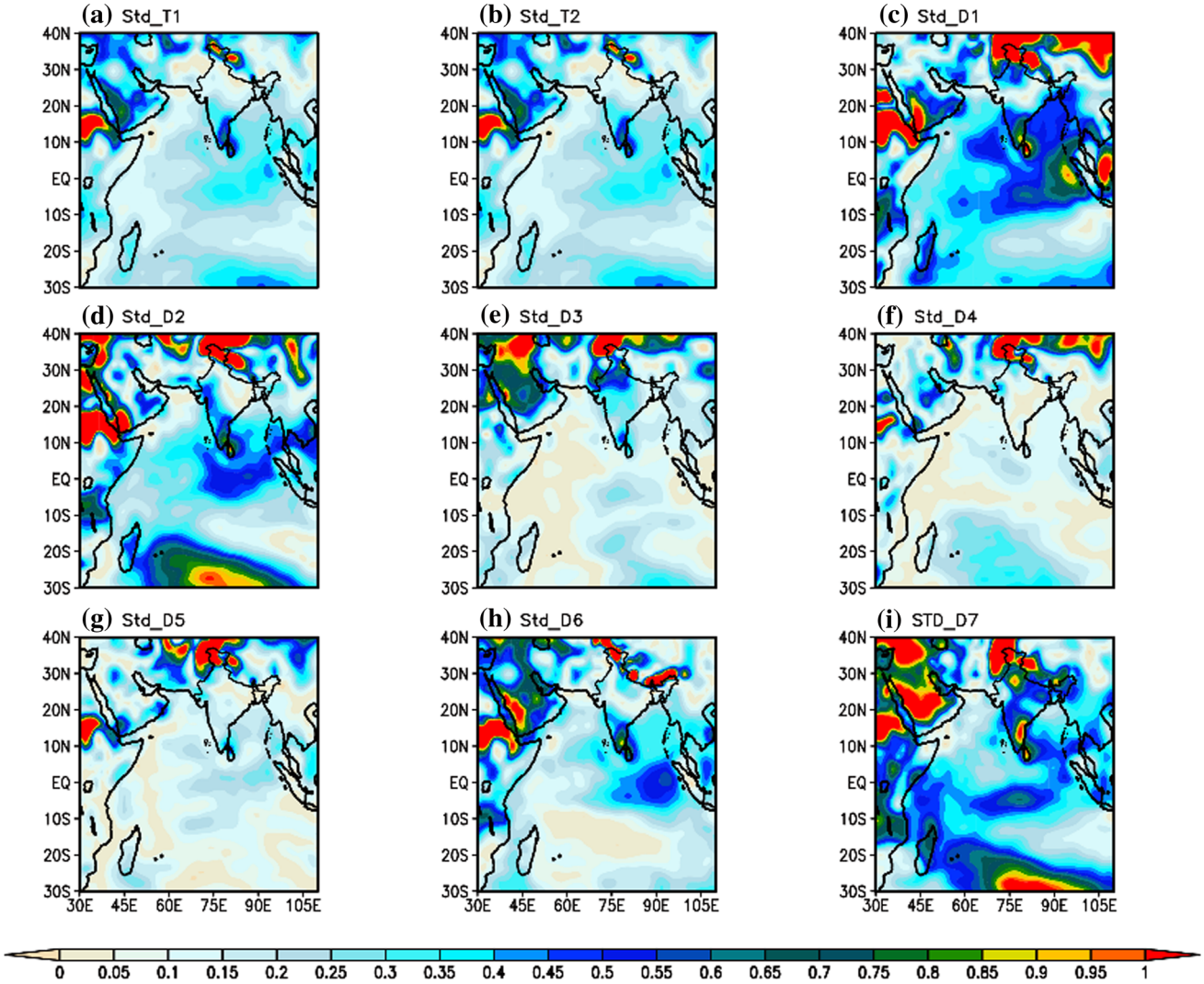

Figure 8. Composite of tricadal and decadal standard deviation (Std) (units are in °C) during monsoon season (1948–2017) for T2m. **(a)** First tricade (Std_T1; 1948–1982), **(b)** recent (Std_T2; 1983–2017) tricade, and **(c–i)** decadal variation of Std for first (Std_D1), second (Std_D2), third (Std_D3), fourth (Std_D4), fifth (Std_D5), sixth (Std_D6) and seventh (Std_D7) decades, respectively.

radiation. The effect of cloud on temperature depends on the balance of cooling (due to reduced solar radiation) and warming (due to reduced outgoing longwave radiation). The climatology of cloud pattern during summer monsoon over India is relatively widespread and plays an important role to study the variation of cloudiness over Indian region. Studies in the past few decades indicate a strong linkage between the type, amount and diurnal variation of the cloud pattern and the rainfall. The mean cloud cover, early-late phase (statistically significant with student's *t*-test), and decadal cloud cover anomaly over Indian region during summer monsoon season are depicted in figure 5. The spatial plot of cloud cover is explained with the help of OLR as well as precipitation because the average plot of cloud cover and precipitation was found to be almost similar pattern over Indian region. The mean climatology of cloud cover is well distributed over ocean region, large amount of cloud cover indicated convective activity and low OLR. Further early-late phase cloud cover anomaly, negative anomaly is found over AS, BoB, southern region, (0.4–1.4%) whereas less positive anomaly over north-east (Lohmann and Feichter 2005), central and north-west region. Further, the decadal anomaly of cloud cover is depicted in the rest part (figure 5) having more variations over EIO and landmass of India during monsoon season. In recent years, India has experienced a reduction in low cloud, perhaps due to an increase in anthropogenic aerosols like black carbon or soot, which can absorb more sunlight (Huang *et al.* 2020). The enhancement of

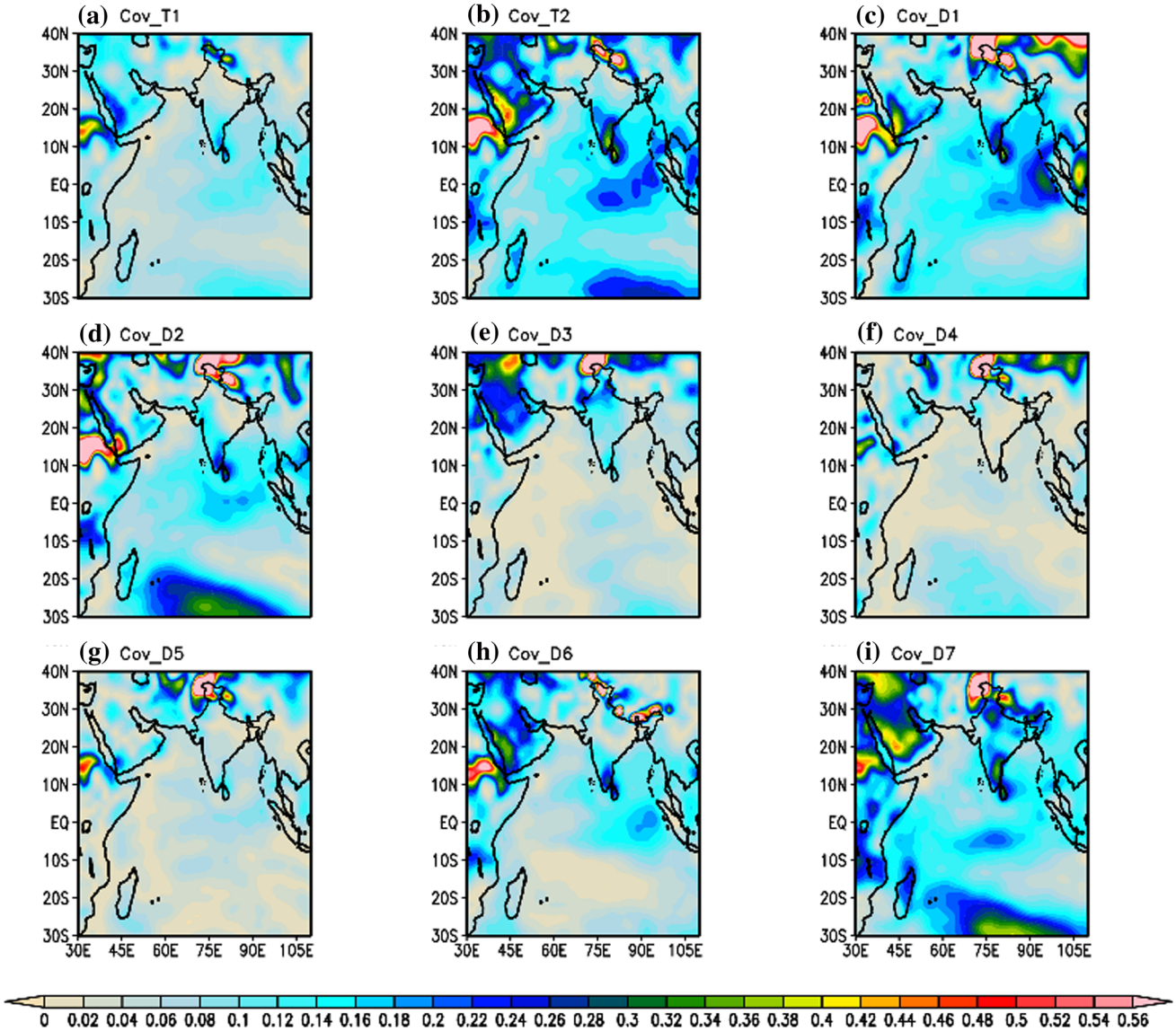

Figure 9. (**a–i**) Same as figure 8, but computed for coefficient of variation (COV) (%) of T2m.

cloudiness is very important over the AS and BoB which manifests the strengthening of LLJ and therefore the monsoon progression (Bhatla *et al.* 2016). They further suggested that insufficient humidity in the AS prevents the development of large systems along the coastlines.

3.6 *Climatology and epochal changes of outgoing long wave radiation*

The climatology of OLR over Indian region was analysed for a relationship with the basic meteorological parameters (pressure, temperature, rainfall, wind vector and cloud cover) during the summer monsoon season. The spatial distribution of OLR composite mean, early-late phase and decadal anomaly were regionally dependent with both excess as well as deficient monsoon rainfall (figure 6). From figure 6(a), climatology of OLR lower than 240 W/m^2 indicate the presence of high cloud cover and also show the probability of precipitation. The OLR pattern closely follows the total cloud cover (figure 5). The variation of OLR is maximum over northwestern region, further decreases over central India and peninsular region, and minimum OLR is found over northeast as well as Himalayan regions. The distribution of early-late phase anomaly of OLR is statistically significant with student's *t*-test at 99% level. The positive anomaly (2–8 W/m^2) is seen over the entire region except Jammu and Kashmir, some parts of Himachal Pradesh and the adjoining region of Nepal

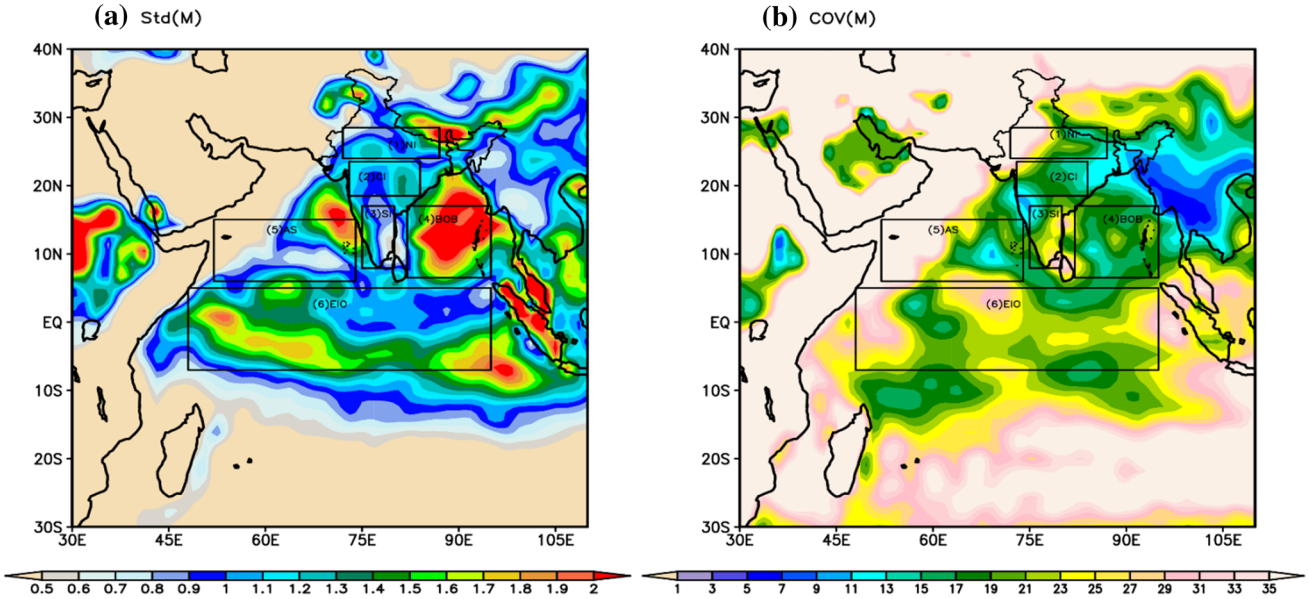

Figure 10. (**a, b**) Same as figure 7, but computed for composite of precipitation (units are in mm/day).

(negative anomaly –3 to –6 W/m^2). Figure 6(c–h) depicts the variation of OLR decadal anomaly from 1948 to 2017. It is once again noticed that significant changes for distribution of decadal OLR anomaly pattern consistently increases in recent decadal anomaly; the reason behind that is the increase in convection and also the dependence of cloud cover (Rajeevan *et al.* 2000; Krishnamurthy and Shukla 2008). The spatial variation of OLR over EIO depended on the distribution of cloud cover and also related to variation in precipitation due to relatively stable surface temperature. Since over the tropical region, intense convection represents low OLR, whereas cloud-free regions represent relatively high OLR (Prasad and Bansod 2000; Mohanty *et al.* 2005). Thus, the distribution of OLR is very useful in understanding the dynamics of ISM in changing climate.

3.7 *Spatial distribution of Std and CV for surface temperature and precipitation*

Significant changes in the surface meteorological parameters are observed over both lands as well as ocean region. Parameters such as variability become important where some of the controlling components of monsoon are prominent during JJAS in changing climate. Because of the large spatial scales involved and the high variability that is inherent to temperature and precipitation, variability was quantified by the Std of mean, early-late phase and decadal distribution as well as the CV (figures 8 and 9). Figure 7 shows the spatial distribution of standard deviation and CV of surface temperature during monsoon season from 1948 to 2017 over Indian region mainly in six selected regions. These regions are selected because of the major changes observed in spatial plot of early-late phase and decadal anomaly from mean of the parameters (surface pressure, surface temperature, precipitation, wind, cloud cover and OLR) during ISM (figures 1–6). The six selected regions NI, CI, SI, AS, BoB and EIO where higher variability was observed during early-late phase and decadal anomalies. The seasonal mean temperature over Indian region varied from 24.416 to 25.818°C, average temperature 25.016°C and Std 0.342 during 70 years. For Std (figure 7a), surface temperature variability is 0.25–0.35°, over AS, BoB (0.25–0.45°C) and over eastern EIO (0.35–0.45°C), more variability than western EIO (0.25–0.35°C) region and high variability of >0.45°C observed over CI, while NI and SI show variability between 0.55–0.75°C and 0.45–0.75°C. The CV, a statistical measure of the dispersion of data points in a data series around the mean, was computed for average, early-late phase and decadal temperature in order to investigate the spatial pattern of epochal variability of summer monsoon surface temperature over the Indian region. The CV varied over western side of NI and EIO more than eastern part from 0.18–0.24% to 0.06–0.2% (eastern and western part of EIO) in figure 7(b). The variability of CV is in increasing pattern over AS (0.08–0.12%), BoB

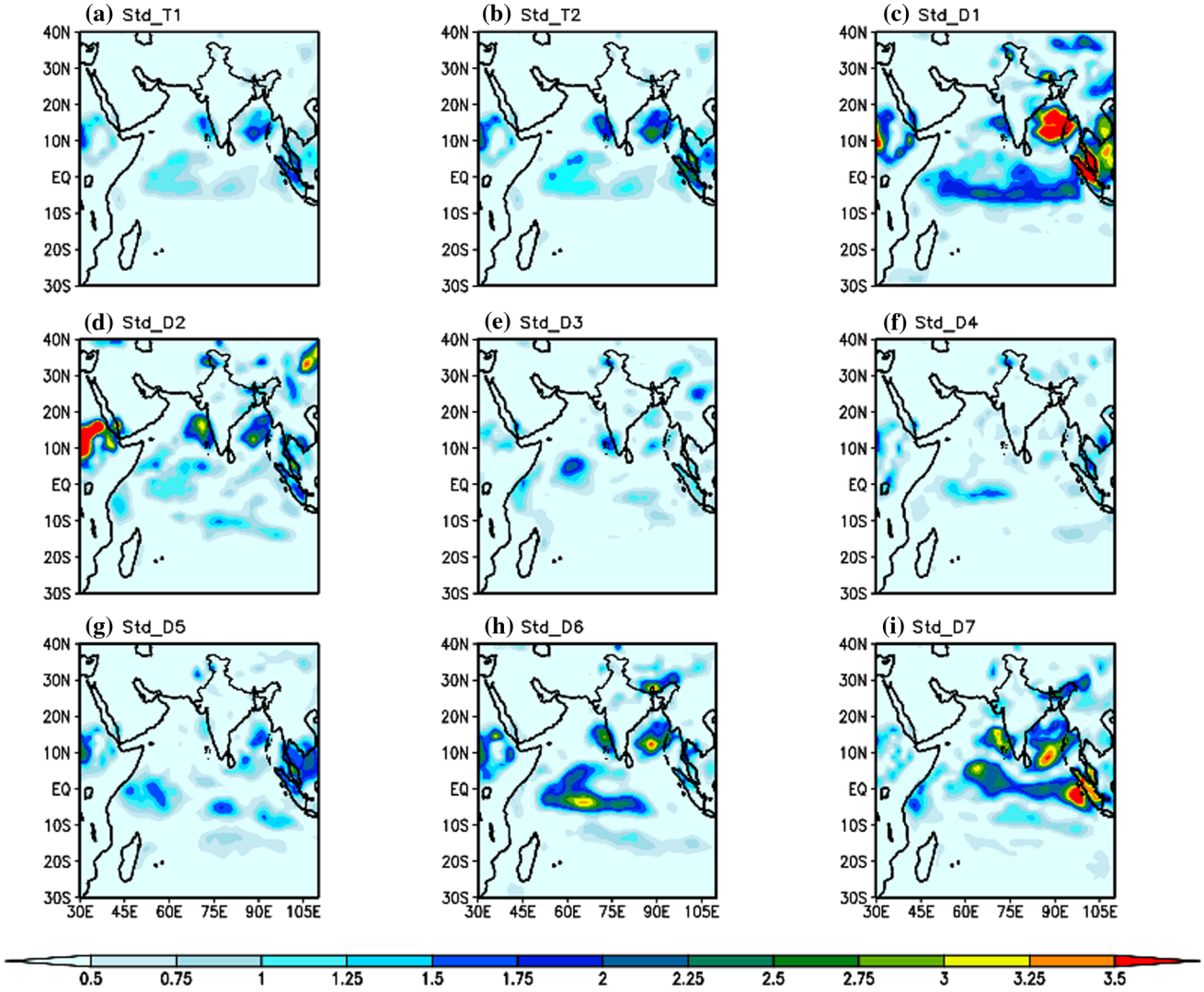

Figure 11. (**a–i**) Same as figure 8, but for precipitation (units are in mm/day).

(0.1–0.14%), CI (0.14–0.18%) and SI (0.14–0.22%). The early-late phase and inter-decadal variation of Std of surface temperature as well as the CV in the monsoon season was more during 1948–1957, 1958–1967, 1998–2007 and 2008–2017 decades, out of which the highest was 0.65°C and 0.24% in 2008–2017 (figures 8 and 9). This indicates low surface temperature variability over oceanic region and high in the land region. While considering the mean seasonal rainfall, advantageous measure to understand variability is CV which is supported in the previous studies by Duncan *et al.* (2013).

A zonal pattern in the distribution of the average precipitation of Std and CV is also clear (figure 6). From figures 10–12, the variation of Std and CV in precipitation is more than in surface temperature. From figure 10, Std and CV in the study area were higher (AS, BoB, EIO) for the seasonal mean period 1948–2017 and mildly lower over the land region (NI, CI, SI). This indicates that Std of rainfall variability over eastern part of NI (1.2–1.8 mm/day) is more than the western part of NI (0.9–1.3 mm/day), whereas over CI and NI changes between 1–1.5 and 0.8–1.1 mm/day. The Std values over eastern part of AS (1.1–1.9 mm/day) are higher than western part (0.6–0.9 mm/day). Further, the variation of Std over IO is 0.8–1.9 mm/day while highest variability 1.0–2.0 mm/day has been reported over BoB region (figure 10a). From figure 10(b), the variability of CV for rainfall over western (W) side of NI and AS is more than the eastern (E) part of NI and AS from 27 to 35% and 13–27% (W and E part of NI), and 25–35% and 9–25% (W and E of AS). Furthermore, variability of CV is also in increasing pattern over BoB (11–23%), CI (11–27%), SI (9–30%) and IO (15–35%). The early-late phase and decadal

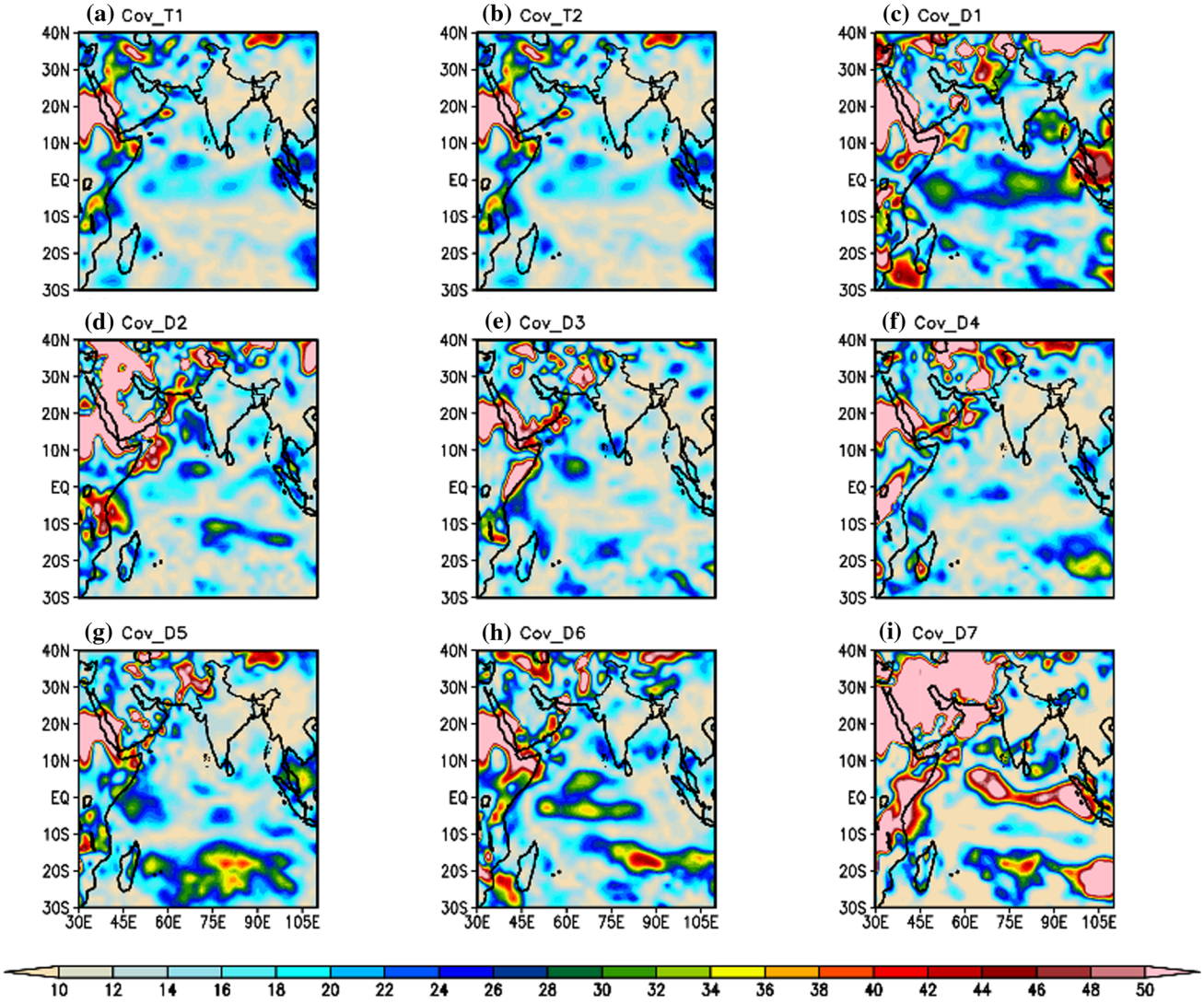

Figure 12. (**a–i**) Same as figure 9, but computed for precipitation (%).

Table 1. *Mann–Kendall trend test analysis for surface temperature (°C) over all India and its different regions during summer monsoon (1948–2017).*

Region[#]	Average surface temperature	Standard deviation	Kendall's tau	Sen's slope	Remark	Trend
AI	25.01	0.34	0.487	0.034	Significant**	Increasing
NI	27.40	0.54	−0.10	−0.006	Not significant	Decreasing
CI	26.24	0.47	0.012	0.0011	Not significant	Increasing
SI	25.98	0.57	0.035	0.0023	Significant*	Increasing
AS	27.18	0.35	0.087	0.0061	Not significant	Increasing
BoB	28.07	0.40	0.030	0.0036	Not significant	Increasing
EIO	26.90	0.37	0.069	0.0059	Not significant	Increasing

[#] AI: All India, NI: North India, CI: Central India, SI: Southern India, AS: Arabian Sea, BoB: Bay of Bengal, EIO: Equatorial Indian Ocean.

* 90% level of significance; ** 95% level of significance.

Table 2. *Mann–Kendall trend test analysis for precipitation (mm/day) over all India and its different regions during summer monsoon (1948–2017).*

Region[#]	Average precipitation	Standard deviation	Coefficient of variation (%)	Kendall's tau	Sen's slope	Remark	Trend
AI	4.20	0.62	14.56	0.48	–0.032	Significant**	Decreasing
NI	5.58	0.84	15.28	0.14	0.013	Not significant	Increasing
CI	6.50	0.92	14.21	–0.35	0.002	Not significant	Increasing
SI	4.63	0.84	18.25	–0.004	0.006	Significant*	Increasing
AS	4.12	0.61	14.87	–0.29	–0.028	Not significant	Decreasing
BoB	10.38	1.70	16.43	–0.67	–0.040	Not significant	Decreasing
EIO	6.06	0.96	15.83	0.51	0.036	Not significant	Increasing

[#] AI: All India, NI: North India, CI: Central India, SI: Southern India, AS: Arabian Sea, BoB: Bay of Bengal, EIO: Equatorial Indian Ocean.

* 90% level of significance; ** 95% level of significance.

variation of spatial distribution of Std for rainfall during the monsoon season are depicted in figure 11, major variations are found over sea areas, i.e., AS, BoB and IO. In the first half from mean (T1) (figure 11a), (1948–1982), variability of Std for rainfall over AS is 0.75–1.5 mm/day, BoB (0.75–2.0 mm/day) and IO (0.5–1.5 mm/day); further during the second half from mean (T2) (figure 11b), (1983–2017) over AS and IO (0.75–2.0 mm/day) and higher over BoB (0.75–2.25 mm/day). Some recent analyses carried out by Jin and Wang (2017) found that the significant reduction in precipitation patterns in central and SI threatens water security. For decadal variation of Std, higher variability is depicted in first, second, sixth and seventh decades (1948–1957, 1958–1967, 1998–2007 and 2008–2017, figure 11c, d, h, i) out of which the highest Std was 3.5 mm/day and CV, 62% in 2008–2017 decade over eastern part of IO near Sumatra (figure 12). This indicates that in 1948–1957 and 2008–2017, the rainfall variability was high compared to that in other decades (1958–1967, 1968–1977, 1978–1987, 1998–2007). This study shows that the Std and CV are useful in characterizing the variation of precipitation, which is a highly variable meteorological parameter in changing climate both temporally and spatially.

The major variation identified in six significant sectors/regions, namely NI, CI, SI, AS, BoB and EIO are shown in figures 7 and 10. The boxes were chosen to cover the regions where some of the governing components of the monsoon (such as the differential heating and cooling of land and ocean water regions, LLJ in the AS, the shift of the position of ITCZ as monsoon trough over the IGP, monsoonal disturbances in the BoB, Southern Oscillation and IOD in EIO) are noticeable and regions where significant major changes occur in meteorological parameters during summer monsoon in changing climate.

3.8 *Mann–Kendall trend and Sen's slope analysis for surface temperature and precipitation over six selected regions*

In present study some statistical parameters such as mean, Std and CV (tables 1 and 2) have been calculated to analyze the behavior of reanalysis surface temperature and rainfall over the region of interest. Figure 13 explains the surface temperature and rainfall pattern over NI, CI, AS, BoB and EIO which reveals higher variability during summer monsoon season. As a result, this study covers both variability and trend analysis (based on historical data of 1948–2017 years) based on non-parametric methods such as M–K test.

The surface temperature averaged over the country (India) has a significant increasing trend during the past decades. Consider standardized anomaly indices of surface temperature and increasing/decreasing trend of temperature is inversely related with precipitation mainly over all India, NI, AS and BoB region during summer monsoon season. The variation of standardized precipitation anomaly over AS and BoB consistently decreases due to weakening of monsoonal wind strength in changing climate. Whereas the variation of temperature and precipitation over IO region is significantly increasing (figure 13g). The reason behind that is, the increase in temperature and precipitation could arise together as an increase in temperature enhances the capacity of the atmosphere to hold water that in turn steps up the amount of precipitation. Other feasible state

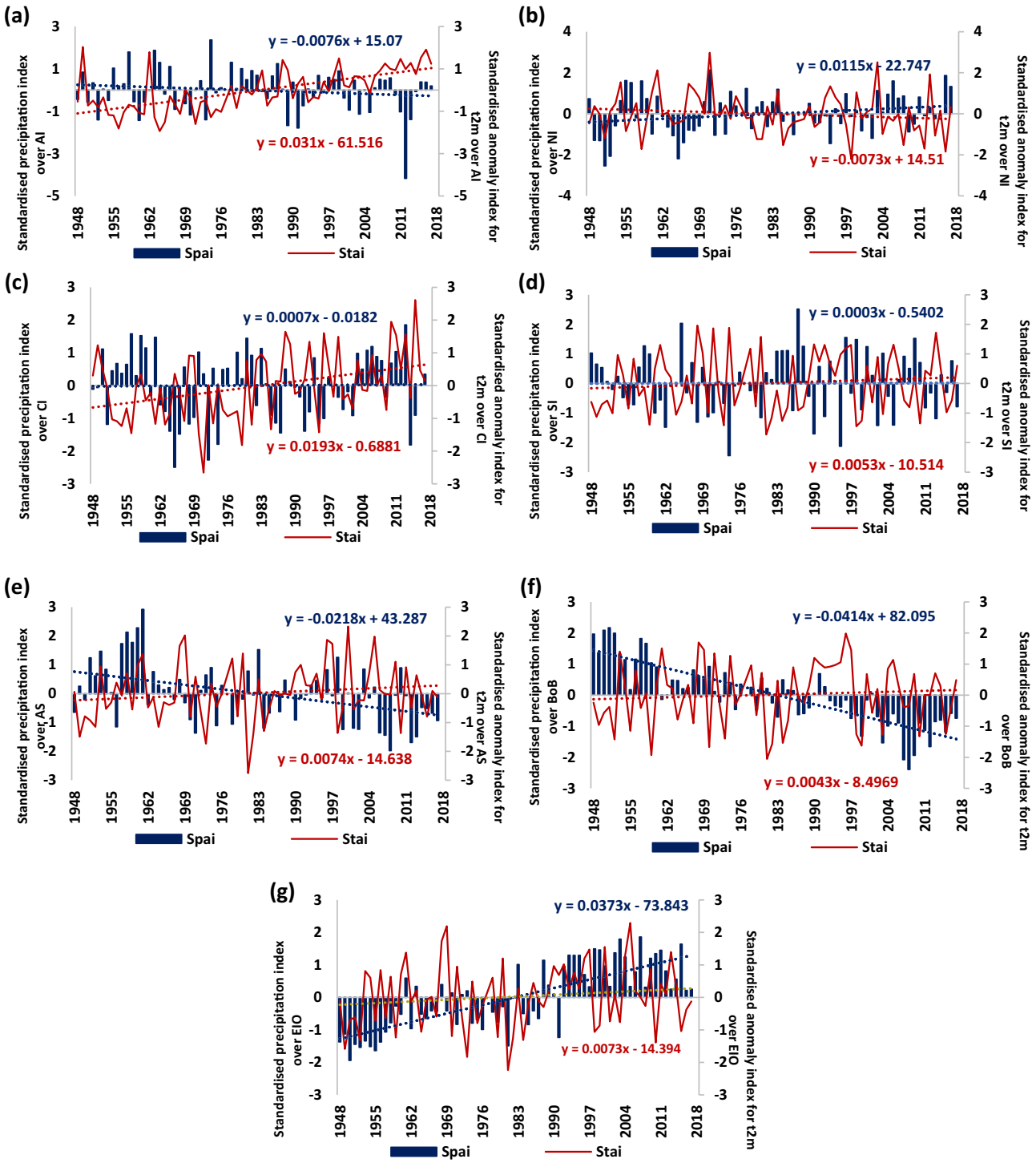

Figure 13. (**a–g**) Composite climatology and trend analysis for standardised precipitation anomaly index (Spai) and standardised anomaly index for T2m (Stai) over **(a)** All India (AI), **(b)** North India (NI), **(c)** Central India (CI), **(d)** Southern India (SI), **(e)** Arabian Sea (AS), **(f)** Bay of Bengal (BoB) and **(g)** Equatorial Indian Ocean (EIO).

behind such a phenomenon could be, changes in the existence of the jet stream which is a narrow band of strong winds in the upper atmosphere that blows west to east but often moves to north and south. Some studies (Lohmann and Feichter 2005; Wang *et al.* 2009) analyze that cooling of Indian continent and northern part of EIO by certain aerosols is linked to the weakening of the north–south surface temperature gradients and decrease in monsoon rainfall.

Trend analysis and M–K test further applied a simple nonparametric procedure developed by Sen

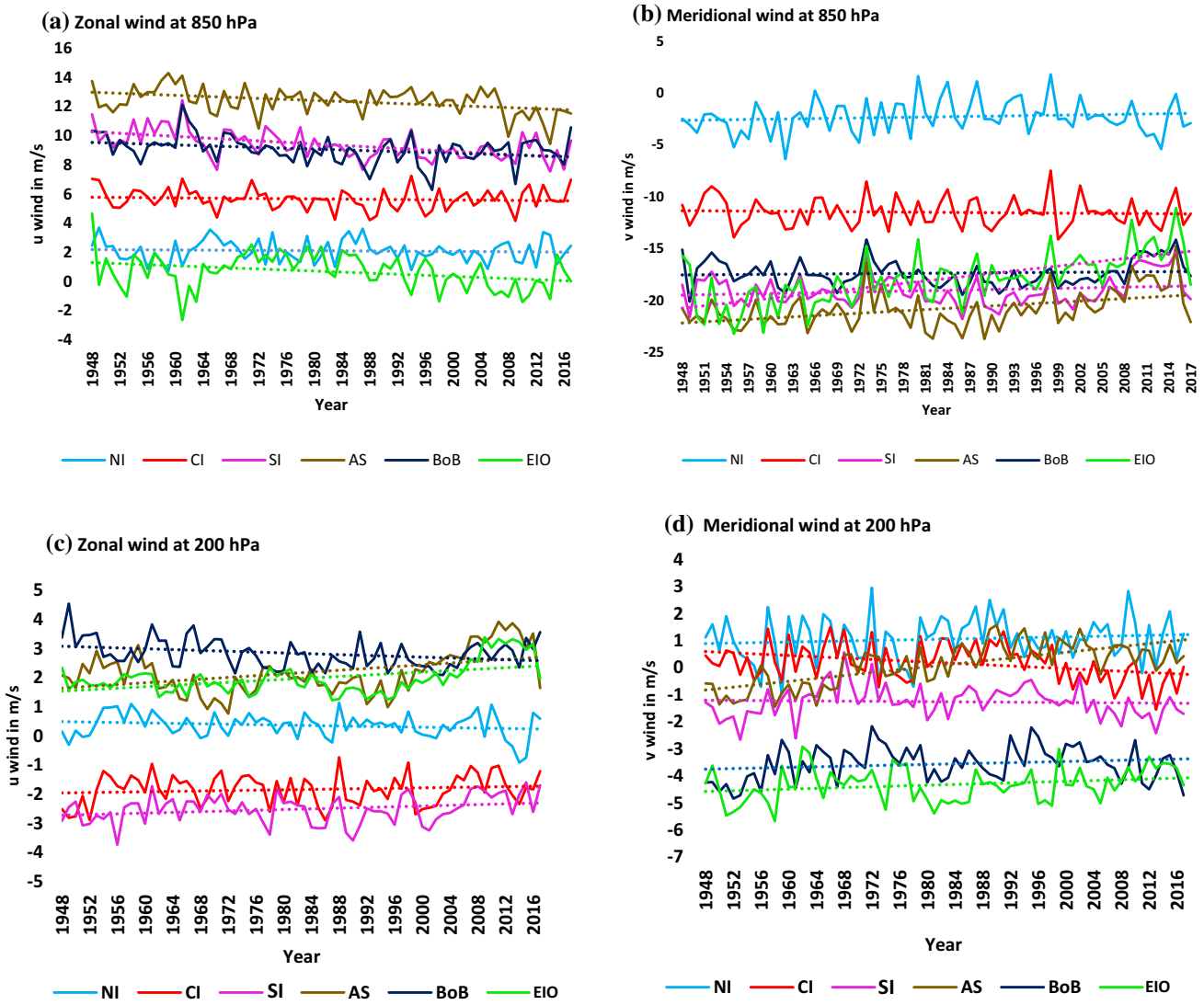

Figure 14. Climatological mean of zonal (u) and meridional (v) wind (in m/s) at 850 and 200 hPa from 1948 to 2017 during summer monsoon season over different regions. **(a)** Zonal wind distribution at 850 hPa, **(b)** temporal variation of meridional wind at 850 hPa, **(c)** temporal variation of zonal wind at 200 hPa and **(d)** temporal variation of meridional wind at 200 hPa. Regions: NI: North India, CI: Central India, SI: Southern India, AS: Arabian Sea, BoB: Bay of Bengal, EIO: Equatorial Indian ocean.

(1968) and estimated the slopes present in the trend. The Sen's slope agrees with the M–K test, i.e., positive value as an indicator of increasing trend. Figure 13(a) also shows the general increasing/decreasing trend for average surface temperature/precipitation respectively, over Indian region during summer monsoon season, where the equation of linear regression shows positive/negative Sen's slope value (0.0344 and –0.0318). It is therefore recommended that the variability of temperature increases, while precipitation decreases in changing climate. Further temporal analysis of M–K test was applied over six selected regions (NI, CI, SI, AS, BoB and EIO) where major spatial variability is observed. Regarding temperature, trends found for average temperature data on monsoon season basis from 1948 to 2017 are not statistically significant except SI. As a result of surface temperature, trend analysis is statistically significant at 90% and 95% confidence limit with an increasing trend over SI and AI, respectively (table 1). The Sen's slope agrees with M–K test result of positive value (0.024) as an indicator of increasing trend. However, the increase is insignificant because the computed value is greater than the significance level. Sen's estimate as shown indicates an increase in the trend of average temperature. On the contrary, the trend analysis result of surface temperature over the rest of four regions is

Table 3. *Mann–Kendall trend test analysis for zonal wind (m/s) at 850 and 200 hPa over all India and its different regions during summer monsoon (1948–2017).*

Region[#]	u wind at 850 hPa	SD	Sen's slope	*P* value	Remark	u wind at 200 hPa	SD	Sen's slope	*P* value	Remark
NI	2.10	0.76	–0.003	0.633	Not significant	2.47	1.38	0.0075	0.53	Not significant
CI	5.66	0.71	–0.004	0.40	Not significant	–11.5	1.40	–0.0046	0.54	Not significant
SI	9.37	0.97	–0.026	0.00002	Significant**	–19.02	1.43	0.0086	0.33	Not significant
AS	12.3	0.91	–0.017	0.003	Significant**	–20.8	1.80	0.035	0.0002	Significant**
BoB	9.04	0.97	–0.012	0.023	Significant**	–17.36	1.26	–0.0002	0.98	Not significant
EIO	1.12	0.81	–0.021	0.006	Significant*	17.98	2.50	0.085	0.0005	Significant**

[#] NI: North India, CI: Central India, SI: Southern India, AS: Arabian Sea, BoB: Bay of Bengal, EIO: Equatorial Indian Ocean.
* 90% level of significance; ** 95% level of significance.

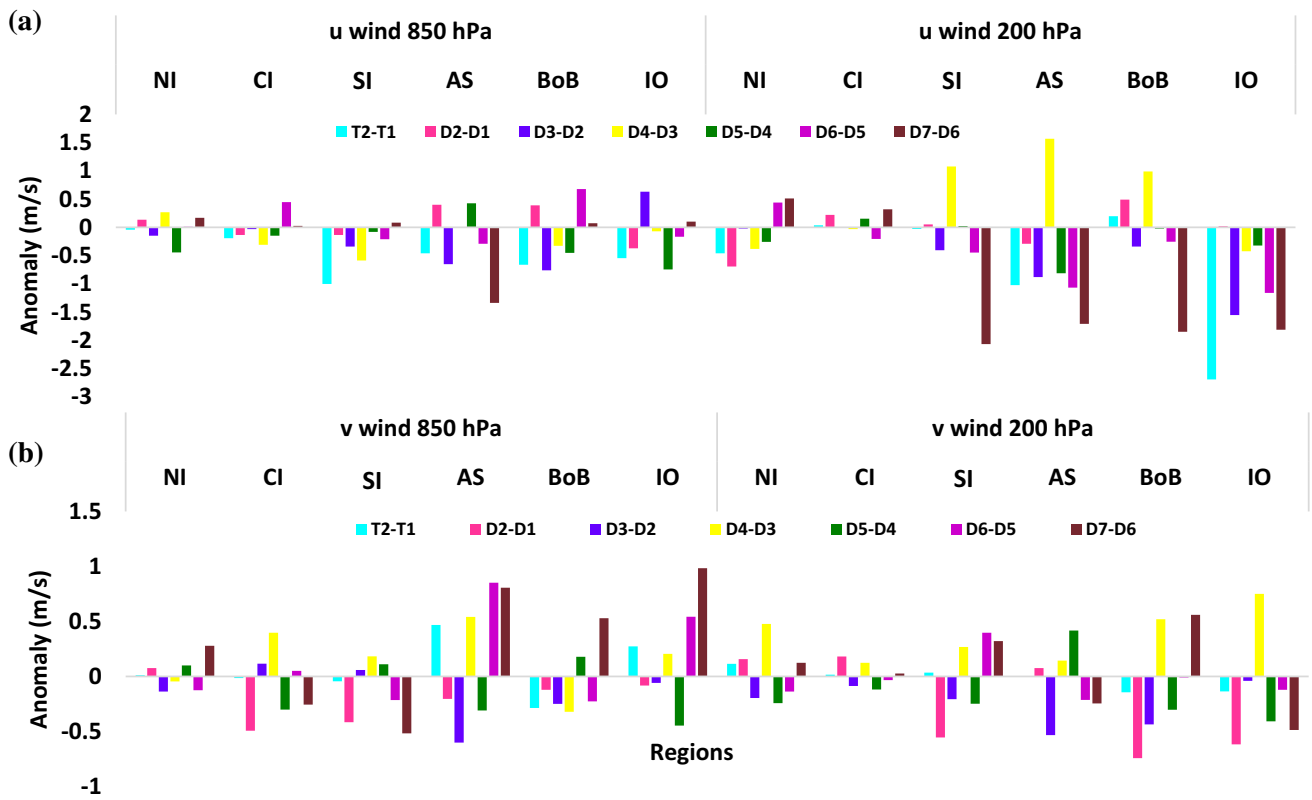

Figure 15. (**a**, **b**) Tricadal and multidecadal fluctuation in the speed (in m/s) of zonal (u) and meridional (v) wind during 1948–2017. Regions: NI: North India, CI: Central India, SI: Southern India, AS: Arabian Sea, BoB: Bay of Bengal, EIO: Equatorial Indian Ocean. Whereas T2–T1 = tricadal anomaly from recent (T2: 1983–2017) to previous tricade (T1: 1948–1982). Decadal anomaly of wind from second (D2: 1958–1967) to first (D1: 1948–1957) decade: D2–D1, D3–D2: third (D3: 1968–1977) and second, D4–D3: fourth (D4: 1978–1987) and third, D5–D4: fifth (D5: 1988–1997) and fourth, D6–D5: sixth (D6: 1998–2007) and fifth, D7–D6: seventh (D7: 2008–2017) and sixth decades, respectively.

not statistically significant with increasing trend over AS, BoB, EIO with Sen's slope 0.0061, 0.0035, 0.0059, respectively. A fitting of linear trend lines shows that there is a decreasing temperature trend for NI (Sen's slope –0.0065). The rise in temperature patterns can result in intense heat waves that could be challenging and supported in the previous study by Dash *et al.* (2007). These plots graphically describe the statistical distribution in a way that is easy to understand for a wide range of users. As the temperature has a crucial impact on water cycle in the study area, a deep understanding of the nature of its occurrence must be carried on. This result shows that global warming study has important impact on the regional climate in the study area for the last seven decades.

Table 4. *Mann–Kendall trend test analysis for meridional wind (m/s) at 850 and 200 hPa over all India and its different regions during summer monsoon (1948–2017).*

Region[#]	v wind at 850 hPa	SD	Sen's slope	*P* value	Remark	v wind at 200 hPa	SD	Sen's slope	*P* value	Remark
NI	0.45	0.31	–0.0028	0.026	Not significant	1.15	0.70	0.0017	0.17	Not significant
CI	–1.84	0.52	0.0028	0.40	Not significant	0.56	0.42	–0.011	0.009	Significant*
SI	2.51	0.50	0.0066	0.51	Not significant	1.28	0.54	–0.0013	0.745	Not significant
AS	2.17	0.74	0.016	0.002	Significant**	0.67	0.40	0.022	0.0004	Significant**
BoB	2.83	0.50	–0.0068	0.03	Significant**	3.5	0.63	0.0067	0.12	Not significant
EIO	1.98	0.54	0.0085	0.007	Significant*	4.3	0.61	0.0087	0.017	Significant**

[#] NI: North India, CI: Central India, SI: Southern India, AS: Arabian Sea, BoB: Bay of Bengal, EIO: Equatorial Indian Ocean.
* 90% level of significance; ** 95% level of significance.

Trends and epochal variability of ISMR for six selected regions and also for all-India are analyzed in detail. For the first time, climatic shift or change point in monsoon rainfall in India is also detected by an established statistical test. The sequential MK test applied in the present study explicitly explains the trends and significance of precipitation during Indian monsoon season. The study explains the trend and significance of precipitation pattern over the studied regions (table 2). The trend lines are also displayed for each of the regions for 70 years. For the Indian region as a whole, the average monsoonal rainfall does not represent any significant trend, while there can be large variations in the regional level during monsoon season, to study the temporal variations of regional rainfall. Understanding the regional trends in ISMR has important implications in developing appropriate adaptation strategies. The statistical analysis of trends for the seasonal mean of precipitation during ISM over different regions of the country is different. The trend analysis of precipitation is statistically significant with decreasing trend (figure 13a, e and f) over AI, AS, BoB with Sen's slope (–0.0257, –0.0059, –0.0287) respectively. There is an increasing precipitation trend for NI, CI and IO (figure 13b, c and h), although the trend over NI and CI are insignificant with Sen's slope value 0.0129 and 0.00257. The trend over IO is statistically significant with Sen's slope value 0.0365. A mechanistic explanation for the trends of seasonal mean rainfall during ISM was done by Dutt *et al.* (2015) and observed that increasing trend of rainfall over IO is due to high convection activity, while the decreasing trend of rainfall over BoB seems to be due to the decreasing trends of low-level wind speed and moisture content. The interaction of EIO with the atmosphere plays an important role in climate variability on both regional and global scales. Therefore, here the analysis of spatio-temporal variation as well as asymmetry trend in precipitation is of great importance to understand the dynamics of ISM in changing climate.

3.9 *Temporal analysis of early-late phase and multidecadal anomaly with Mann–Kendall trend and Sen's slope for zonal and meridional wind at 850 and 200 hPa over six selected regions*

The variation of rainfall and temperature largely depends on the spatio-temporal variation of wind over India and its neighbourhood region. The early-late phase and multi-decadal variation of wind are high due to large variation in the characteristics of synoptic disturbances developing over the AS, BoB and IO. Composite of zonal and meridional wind at 850 and 200 hPa during 1948–2017 is depicted in figure 14(a–d) over NI, CI, SI, AS, BoB and IO. These results show the decreasing trends of seasonal mean of zonal wind at 850 hPa over all regions (table 3) due to weakening of monsoonal LLJ in recent epochs. Decreasing trend of zonal wind at 850 hPa over SI, AS, BoB and IO is statistically significant, decreases at 95% of confidence limit with Sen's slope. Further trend analysis for zonal wind at 200 hPa (figure 14b) shows the positive trend for summer monsoon season over all regions except CI and over AS, IO region statistically significant at 95% of confidence limit. Temporal variation of meridional wind at 850 and 200 hPa has significant increasing trend over AS and EIO during monsoon season (figure 14b and d), whereas rest of the regions (i.e., CI, NI, SI and BoB) depict decreasing trend during the period (table 3). Figure 15 shows the early-late phase and multidecadal fluctuation in the

speed (in m/s) of zonal (u) and meridional (v) wind at 850 and 200 hPa. As evident from figure 15(a), a decreasing trend of T2–T1 and recent decadal anomaly (D7–D6) were found over all regions for zonal wind speed at 850 and 200 hPa. In contrast to early-late phase and multidecadal anomaly for meridional wind at 850 and 200 hPa levels, insignificant increasing/decreasing observed for all regions (table 4). Figure 15(b) shows recent decadal anomaly for meridional wind at 850 hPa having positive anomaly over oceanic region due to having moisture and latent heat associated with LLJ. The meridional wind at 200 hPa have shown positive anomaly over SI and BoB which is associated with LLJ (as discussed earlier) whereas negative anomaly has been observed over AS and IO. Due to decreasing trend of T2–T1 and recent decadal anomaly of the zonal wind passing through AS and SI, meridional wind also weakens which might manifest the monsoonal drought conditions in the future (Joseph and Simon 2005).

4. Conclusions

The present study clearly demonstrates the significant changes in surface meteorological parameters (temperature, pressure, precipitation, wind, OLR and cloud cover) over NI, CI, SI, AS, BoB and IO region during the ISM from 1948 to 2017. In the early-late phase (T2–T1) anomaly of surface temperature, a warming pattern over southern and some parts of western region and a cooling pattern over northeastern and central region is observed. The surface warming over the BoB region (28–30°C) is found prominent than AS region (26–28°C), because during monsoon season (JJAS) winds are stronger and support the change of heat to deeper layers owing to overturning and turbulent mixing (Shenoi *et al.* 2002). The distribution of wind anomaly is closely associated with temperature, pressure and precipitation anomaly. Further multidecadal anomalies of wind show significant increase in recent decadal anomalies due to the presence of strong westerly, southeasterly and southerly anomalies over the EIO, BoB, AS and adjoining regions. The major variation in surface temperature is found over land region (NI, SI, and CI) rather than AS, BoB, EIO because of the topographical difference in different regions. The increasing trend pattern of average surface temperature over AI and SI is statistically significant with positive Sen's slope, while other regions (CI, AS, BoB, EIO) show insignificant increasing trend. The average rainfall during monsoon season has shown decreasing trends over AS, BoB, although over EIO found an increasing trend. AS and BoB region experience decreasing trend of zonal and meridional wind. Along with significant decreasing anomaly in zonal and meridional at 850 hPa (LLJ) over the SI region, there is an increase break spell tendency in future. Temporal trend of surface temperature, precipitation, zonal and meridional wind in the context of a changing climate is crucial to examine climate-induced changes and in understanding the dynamics of ISM. From the current study, the variations in meteorological parameters and distribution are uneven along with trend analysis examinations, well remarkable over the India region. However, these results are not precise, some are regulated at local scale and demand more investigation during monsoon climate change.

Acknowledgements

The authors acknowledge the University Grants Commission (UGC), India for providing the Research Fellowship for continuing Doctoral study. They also wish to extend special thanks to NCEP/NCAR reanalysis for providing necessary data. Authors express their sincere gratitude to the editor and the reviewers for their valuable suggestions and comments.

Authors statement

RB and PS: Conceptualization, technical guidance and supervision. AM: Data collection and analysis and writing manuscript. SV and MP: Data analysis and review of the manuscript.

References

Ananthakrishnan R and Soman M K 1989 Statistical distribution of daily rainfall and its association with the coefficient of variation of rainfall series; *Int. J. Climatol.* **9(5)** 485–500, https://doi.org/10.1002/joc.3370090504.

Aneesh S and Sijikumar S 2016 Changes in the south Asian monsoon low level jet during recent decades and its role in the monsoon water cycle; *J. Atmos. Sol.-Terr. Phys.* **138** 47–53.

Bhatla R, Gyawali B, Mall R K and Raju P V S 2013 Study of possible linkage of PDO with Indian summer monsoon in relation to QBO; *Vayumandal* **39(1–2)** 40–45.

Bhatla R, Raju P V S, Mall R K and Bist S 2016 Study of surface fluxes during onset of summer monsoon over India; *Int. J. Climatol.* **36(4)** 1821–1832, https://doi.org/10.1002/joc.4462.

Bhatla R, Sharma S, Verma S and Gayawali B 2020 Impact of Pacific Decadal Oscillation in relation to QBO on Indian summer monsoon rainfall; *Arab. J. Geosci.* **13(22)** 1207, https://doi.org/10.1007/s12517-020-06225-6.

Curio J, Schiemannm R, Hodges K I and Turner A G 2019 Climatology of Tibetan Plateau vortices in reanalysis data and a high-resolution global climate model; *J. Clim.* **32(6)** 1933–1950, https://doi.org/10.1175/JCLI-D-18-0021.1.

Dash S K, Jenamani R K, Kalsi S R and Panda S K 2007 Some evidence of climate change in twentieth-century India; *Clim. Change* **5(3)** 299–321, https://doi.org/10.1007/s10584-007-9305-9.

Dong B, Sutton R T, Highwood E J and Wilcox L J 2016 Preferred response of the East Asian summer monsoon to local and non-local anthropogenic sulphur dioxide emissions; *Clim. Dyn.* **46(5–6)** 1733–1751, https://doi.org/10.1007/s00382-015-2671-5.

Duan A, Wang M, Lei Y and Cui Y 2013 Trends in summer rainfall over China associated with the Tibetan Plateau sensible heat source during 1980–2008; *J. Clim.* **26(1)** 261–275.

Duncan J A, Dash J and Atkinson P M 2013 Analysing temporal trends in the Indian Summer Monsoon and its variability at a fine spatial resolution; *Clim. Change* **117(1)** 119–131.

Dutt S, Gupta A K, Clemens S C, Cheng H, Singh R K, Kathayat G and Edwards R L 2015 Abrupt changes in Indian summer monsoon strength during 33,800 to 5500 years BP; *Geophys. Res. Lett.* **42(13)** 5526–5532.

Gadgil S 2000 Monsoon–ocean coupling; *Curr. Sci.* **78**(3) 309–322.

Gadgil S, Vinayachandran P N, Francis P A and Gadgil S 2004 Extremes of the Indian summer monsoon rainfall, ENSO and equatorial Indian Ocean oscillation; *Geophys. Res. Lett.* **31(12)**.

Gocic M and Trajkovic S 2013 Analysis of changes in meteorological variables using Mann–Kendall and Sen's slope estimator statistical tests in Serbia; *Glob. Planet. Change* **100** 172–182.

Goswami B N 2006 The Asian monsoon: Interdecadal variability. In: *The Asian Monsoon*; Springer, Berlin, Heidelberg, pp. 295–327.

Goswami B N, Krishnamurthy V and Annmalai H 1999 A broad-scale circulation index for the interannual variability of the Indian summer monsoon; *Quart. J. Roy. Meteorol. Soc.* **125(554)** 611–633.

Guhathakurta P and Rajeevan M 2008 Trends in the rainfall pattern over India; *Int. J. Climatol.* **28(11)** 1453–1469.

Guhathakurta P, Rajeevan M, Sikka D R and Tyagi A 2015 Observed changes in southwest monsoon rainfall over India during 1901–2011; *Int. J. Climatol.* **35(8)** 1881–1898.

Guo L, Turner A G and Highwood E J 2016 Local and remote impacts of aerosol species on Indian summer monsoon rainfall in a GCM; *J. Clim.* **29(19)** 6937–6955.

Han W, Vialard J, McPhaden M J, Lee T, Masumoto Y, Feng M and De Ruijter W P 2014 Indian Ocean decadal variability: A review; *Bull. Am. Meteorol. Soc.* **95(11)** 1679–1703.

Huang X, Zhou T, Turner A, Dai A, Chen X, Clark R, Jiang J, Man W, Murphy J, Rostron J and Wu B 2020 The recent decline and recovery of Indian summer monsoon rainfall: Relative roles of external forcing and internal variability; *J. Clim.* **33(12)** 5035–5060.

Jin Q and Wang C 2017 A revival of Indian summer monsoon rainfall since 2002; *Nat. Clim. Change* **7(8)** 587–594.

Joseph P V and Sijikumar S 2004 Intraseasonal variability of the low-level jet stream of the Asian summer monsoon; *J. Clim.* **17(7)** 1449–1458.

Joseph P V and Simon A 2005 Weakening trend of the southwest monsoon current through peninsular India from 1950 to the present; *Curr. Sci.* **89(4)** 687–694.

Kalnay E, Kanamitsu M, Kistler R, Collins W, Deaven D, Gandin L, Joseph D *et al.* 1996 The NCEP/NCAR 40-year reanalysis project; *Bull. Am. Meteorol. Soc.* **77(3)** 437–472.

Karmakar N, Chakraborty A and Nanjundiah R S 2017 Space–time evolution of the low- and high-frequency intraseasonal modes of the Indian summer monsoon; *Mon. Wea. Rev.* **145(2)** 413–435.

Kendall M G 1975 *Multivariate analysis*; (Vol. 2), London: Griffin.

Kistler R, Kalnay E, Collins W, Saha S, White G, Woollen J, Chelliah M, Ebisuzaki W, Kanamitsu M, Kousky V, van den Dool H, Jenne R and Fiorino M 2001 The NCEP-NCAR 50-year reanalysis: Monthly means CD-ROM and documentation; *Bull. Am. Meteorol. Soc.* **82** 247–267.

Kothawale D R, Munot A A and Kumar K K 2010 Surface air temperature variability over India during 1901–2007, and its association with ENSO; *Clim. Res.* **42(2)** 89–104.

Kraus E B 1977 Subtropical droughts and cross-equatorial energy transports; *Mon. Wea. Rev.* **105(8)** 1009–1018.

Kripalani R H and Kulkarni A 1997 Rainfall variability over southeast Asia – connections with Indian monsoon and ENSO extremes: New perspectives; *Int. J. Climatol.* **17(11)** 1155–1168.

Krishnamurthy V and Goswami B N 2000 Indian monsoon–ENSO relationship on interdecadal timescale; *J. Clim.* **13(3)** 579–595.

Krishnamurthy V and Shukla J 2008 Seasonal persistence and propagation of intraseasonal patterns over the Indian monsoon region; *Clim. Dyn.* **30(4)** 353–369.

Krishnan R, Ayantika D C, Kumar V and Pokhrel S 2011 The long-lived monsoon depressions of 2006 and their linkage with the Indian Ocean Dipole; *Int. J. Climatol.* **31(9)** 1334–1352.

Krishnan R, Sabin T P, Ayantika D C, Kitoh A, Sugi M, Murakami H, Turner A G, Slingo J M and Rajendran K 2013 Will the South Asian monsoon overturning circulation stabilize any further?; *Clim. Dyn.* **40(1–2)** 187–211.

Kumari A, Kumar P, Dubey A K, Mishra A K and Saharwardi M S 2021 Dynamical and thermodynamical aspects of precipitation events over India; *Int. J. Climatol.*, https://doi.org/10.1002/joc.7409.

Levine R C, Turner A G, Marathayil D and Martin G M 2013 The role of northern Arabian Sea surface temperature biases in CMIP5 model simulations and future projections of Indian summer monsoon rainfall; *Clim. Dyn.* **41(1)** 155–172.

Li Z, Lau W M, Ramanathan V, Wu G, Ding Y, Manoj M G, Liu J, Qian Y, Li J, Zhou T and Fan J 2016 Aerosol and monsoon climate interactions over Asia; *Rev. Geophys.* **54(4)** 866–929.

Lohmann U and Feichter J 2005 Global indirect aerosol effects: A review; *Atmos. Chem. Phys.* **5(3)** 715–737.

Loo Y Y, Billa and Singh A 2015 Effect of climate change on seasonal monsoon in Asia and its impact on the variability of monsoon rainfall in Southeast Asia; *Geosci. Frontiers* **6(6)** 817–823.

Malik A, Brönnimann S, Stickler A, Raible C C, Muthers S, Anet J, Rozanov E and Schmutz W 2017 Decadal to multi-decadal scale variability of Indian summer monsoon rainfall in the coupled ocean-atmosphere-chemistry climate model SOCOL-MPIOM; *Clim. Dyn.* **49(9)** 3551–4372.

Mann H B 1945 Nonparametric tests against trend; *Econometrica* **1** 245–259.

Mishra A K, Dwivedi S and Das S 2020a Role of Arabian Sea warming on the Indian summer monsoon rainfall in a regional climate model; *Int. J. Climatol.* **40(4)** 2226–2238.

Mishra A K, Dwivedi S, Di Sante F and Coppola E 2020b Thermodynamical properties associated with the Indian summer monsoon rainfall using a regional climate model; *Theor. Appl. Climatol.* **141(1)** 587–599.

Mohanty U C, Bhatla R, Raju P V S, Madan O P and Sarkar A 2002 Meteorological fields variability over the Indian seas in pre and summer monsoon months during extreme monsoon season; *Proc. Indian Acad. Sci.* (*Earth Planet. Sci.*) **111(3)** 365–378.

Mohanty U C, Raju P V S and Bhatla R 2005 A study on climatological features of the Asian summer monsoon: Dynamics, energetics and variability; *Pure Appl. Geophys.* **162(8)** 1511–1541.

Mooley D A and Parthasarathy B 1984 Fluctuations in all-India summer monsoon rainfall during 1871–1978; *Clim. Change* **6(3)** 287–301.

Naidu C V, Krishna K M, Rao S R, Kumar O B, Durgalakshmi K and Ramakrishna S S V S 2011 Variations of Indian summer monsoon rainfall induce the weakening of easterly jet stream in the warming environment?; *Global Planet. Change* **75(1–2)** 21–30.

Parthasarathy B, Munot A A and Kothawale D R 1994 All-India monthly and seasonal rainfall series: 1871–1993; *Theor. Appl. Climatol.* **49(4)** 217–224.

Prasad K D and Bansod S D 2000 Interannual variations of outgoing longwave radiation and Indian summer monsoon rainfall; *Int. J. Climatol.* **20(15)** 1955–1964.

Rajeevan M, De U S and Prasad R K 2000 Decadal variation of sea surface temperatures, cloudiness and monsoon depressions in the north Indian Ocean; *Curr. Sci.* **79(3)** 283–285.

Rajeevan M, Pai D S, Kumar R A and Lal B 2007 New statistical models for long-range forecasting of southwest monsoon rainfall over India; *Clim. Dyn.* **28(7–8)** 813–828.

Ross R S, Krishnamurti T N, Pattnaik S and Pai D S 2018 Decadal surface temperature trends in India based on a new high-resolution data set; *Sci. Rep.* **8(1)** 1–10.

Sahana A S, Ghosh S, Ganguly A and Murtugudde R 2015 Shift in Indian summer monsoon onset during 1976/1977; *Environ. Res. Lett.* **10(5)** 054006.

Sen P K 1968 Estimates of the regression coefficient based on Kendall's tau; *J. Am. Stat. Assoc.* **63** 1379–1389.

Shenoi S S, Shankar D and Shetye S R 2002 Differences in heat budgets of the near-surface Arabian Sea and Bay of Bengal: Implications for the summer monsoon; *J. Geophys. Res.*: *Oceans* **107(C6)** 5-1.

Singh P, Vasudevan V, Chowdary J S and Gnanaseelan C 2015 Subseasonal variations of Indian summer monsoon with special emphasis on drought and excess rainfall years; *Int. J. Climatol.* **35(4)** 570–582.

Sinha A, Kathayat G, Cheng H, Breitenbach S F, Berkelhammer M, Mudelsee M, Biswas J and Edwards R L 2015 Trends and oscillations in the Indian summer monsoon rainfall over the last two millennia; *Nat. Commun.* **176(1)** 1–8.

Swapna P, Jyoti J, Krishnan R, Sandeep N and Griffies S M 2017 Multidecadal weakening of Indian summer monsoon circulation induces an increasing northern Indian Ocean sea level; *Geophys. Res. Lett.* **44(20)** 10–560.

Trenberth K E 2011 Changes in precipitation with climate change; *Clim. Res.* **47(1–2)** 123–138.

Turner A G and Annamalai H 2012 Climate change and the South Asian summer monsoon; *Nat. Clim. Change* **2(8)** 587–595.

Vidya P J, Ravichandran M, Subeesh M P, Chatterjee S and Nuncio M 2020 Global warming hiatus contributed weakening of the Mascarene High in the Southern Indian Ocean; *Sci. Rep.* **10(1)** 1–9.

Wang C, Kim D, Ekman A M, Barth M C and Rasch P J 2009 Impact of anthropogenic aerosols on Indian summer monsoon; *Geophys. Res. Lett.* **36(21)**.

Yanai M and Tomita T 1998 Seasonal and interannual variability of atmospheric heat sources and moisture sinks as determined from NCEP–NCAR reanalysis; *J. Clim.* **11(3)** 463–482.

Corresponding editor: Kavirajan Rajendran